Survival of the littlest: improving preterm outcomes through metabolomics and microsampling

Thangavelu, M.U.

CHAPTER II

Maternal Urinary Metabolomic Signatures Preceding Spontaneous Preterm Birth: A Pilot Study

Based on:

Maternal urinary metabolomic signatures preceding spontaneous preterm birth: A pilot study

*Manchu Umarani Thangavelu, *Emma Ronde, Lieke Lamont, Hyung L. Elfrink, Amy Harms, Yolanda B. de Rijke, Arie Franx, Tim G. J. de Meij, Alida Kindt, Irwin K.M. Reiss, Sam Schoenmakers and Thomas Hankemeier

Scientific Reports (2025)
https://doi.org/10.1038/s41598-025-28436-1

*Shared first authors

Abstract

The etiological heterogeneity of spontaneous preterm birth (sPTB) complicates PTB risk prediction and management. Accurate risk stratification at clinical suspicion is critical to administer life-saving interventions for fetuses at genuine risk, while avoiding unnecessary treatments in pregnancies progressing to term to mitigate long-term complications. Current tools lack predictive accuracy, with 40% of suspected PTB delivering at term. This pilot study investigated signaling lipids as potential biomarkers for sPTB. Prospectively collected midstream urine of 30 women with imminent PTB were retrospectively classified into preterm without chorioamnionitis, preterm with chorioamnionitis, and term, and analyzed using liquid-chromatography mass-spectrometry. Overall-preterm vs term analysis revealed reduced lipoxygenase- and cytochrome P450-derived oxylipins in the preterm group, suggesting impaired inflammation resolution. Pairwise comparisons showed that these differences were primarily driven by the non-infectious preterm group. Notably, 8,9-DiHETrE and 9-HODE emerged as promising etiology-independent biomarkers for sPTB. Furthermore, oxidative stress dominated non-infectious sPTB cases, while inflammatory cascades characterized the infectious cases. A predictive model incorporating 9-HODE and vaginal discharge demonstrated the ability (AUC 84.2%, sensitivity 73.7%, specificity 88.9%) to differentiate between women delivering preterm and at term. These findings highlight the potential of urinary metabolomics as a non-invasive tool to unravel sPTB pathophysiology and enhance risk prediction.

1. Introduction

Preterm birth (PTB), defined as delivery before 37+0 weeks of gestation, is the leading cause of perinatal mortality and morbidity globally, affecting approximately 10% of all live births annually.[1] PTB has a multifactorial origin, involving a complex interplay of maternal, fetal, and environmental factors.[2] PTB can be categorized into (i) spontaneous PTB (sPTB), which encompasses spontaneous preterm labor with intact membranes or preterm premature rupture of membranes (PPROM), irrespective of eventual mode of delivery, and (ii) iatrogenic PTB (iPTB), wherein delivery is medically indicated due to maternal or fetal complications, through labor induction or pre-labor cesarean section.[3] Developments in obstetric care, including improved monitoring and management of high-risk pregnancies for both maternal and fetal risk, have contributed to an increase in iPTB and a relative decline in sPTB.[4,5] sPTB is often associated with inflammation, maternal infections such as chorioamnionitis and urinary tract infection, uterine overdistension, or cervical insufficiency, while iPTB are frequently driven by maternal conditions such as hypertensive and placental disorders of pregnancy, fetal conditions such as fetal growth restriction, or a combination of both.[3,6] Often, causes of iPTB are identifiable in advance, enabling clinicians to make informed decisions regarding the timing of delivery, balancing the risks of prematurity against potential complications of continuing the pregnancy. However, the mechanisms leading to sPTB remain poorly understood, posing a substantial challenge in their accurate prediction, effective prevention, and timely initiation of treatment.[2]

Early identification and accurate risk stratification of women at risk of sPTB is crucial for facilitating timely interventions to prolong pregnancy, providing sufficient time for fetal interventions to optimize their preparation for preterm delivery and reduce the risks of adverse neonatal outcomes. Depending on the timing during pregnancy, key interventions include targeted therapies such as cervical cerclage and progesterone for women presenting with a short cervix or a history of PTB, antibiotics to manage maternal bacterial vaginosis or infection, maternal administration of antenatal corticosteroids to accelerate fetal lung maturity, magnesium sulphate for fetal neuroprotection, and additional tocolytics to allow administration of fetal therapy.[7] Currently, women at high risk of PTB are identified through an assessment of predisposing factors, including maternal and obstetric history, demographic determinants, and behavioral and environmental influences, as well as clinical evaluation of imminent PTB using diagnostic tools such as cervical length screening, fetal fibronectin testing, and biomarkers of inflammation, such as C-Reactive Protein (CRP).[8,9] However, these approaches are constrained by their moderate predictive accuracy and limited universal applicability.[10] Data from randomized clinical trials and population-based studies have shown that nearly 40% of women diagnosed with imminent PTB and exposed to early antenatal corticosteroids, ultimately deliver at term, highlighting the inadequacy of current

tools in accurately predicting sPTB.[11] The timing of corticosteroid administration is critical to maximize efficacy, with optimal outcomes and reduced fetal side effects achieved when administered 2-7 days prior to delivery.[12] However, unnecessary fetal exposure to corticosteroids in pregnancies that will ultimately end at term is associated with long-term cognitive and behavioral disorders, emphasizing the need for cautious use.[13–16] Furthermore, unnecessary hospital admissions contribute to increased healthcare expenditures and impose a burden on hospital resources. Therefore, methods to accurately predict sPTB are urgently needed to enable timely interventions in women at genuine risk while minimizing unnecessary maternal admission and fetal treatment for those ultimately delivering at term.

The vaginal microbiome has emerged as a promising source of potential predictive biomarkers of PTBs, as it has been shown to differ between pregnancies resulting in term and PTBs, with distinct microbial profiles identifiable as early as the first trimester.[17] Consequently, volatile organic compounds (VOCs), which are the metabolic end-products of biochemical processes such as microbial activity, inflammation, and oxidative stress, are emerging as a promising tool for the prediction of sPTB.[18–20] VOC analysis provides a non-invasive approach to capture microbiome composition, host responses, and their dynamic interactions, offering valuable insights into the metabolic disturbances associated with PTB.[20,21] In a prospective observational cohort study by Lacey *et al*., VOCs derived from vaginal swabs collected in the mid-trimester demonstrated moderate predictive capability (AUC 0.79) for sPTB, with predictive accuracy increasing in samples taken closer to delivery (AUC 0.84).[21] Similarly, in our previous study, urinary VOC analysis revealed distinct profiles between women admitted for imminent preterm birth who delivered preterm (28+0 to 36+6) and those who progressed to term (AUC 0.70). In addition, the urinary VOC profiling proved effective in distinguishing sPTB cases with chorioamnionitis (AUC 0.72) or urinary tract infections (AUC 0.97) from those without these complications.[19] While VOC analysis has demonstrated utility in sPTB prediction and identification of associated infections by providing snapshots of metabolic disturbances, it is inherently limited in its ability to elucidate the molecular mechanisms driving these disturbances.

Signaling lipids, key regulators of inflammation, immune response, and vascular function, offer a powerful framework for deciphering the mechanistic pathways driving sPTB, as a substantial proportion of sPTB cases are associated with inflammation, whether sterile or caused by bacterial infections.[3,22–25] These bioactive molecules encompass a diverse array of compound classes, including oxylipins, free fatty acids (FAs), lysophospholipids, endocannabinoids, and bile acids. Oxylipins, derived from the oxygenation of polyunsaturated FAs either enzymatically through cytochrome P450 (CYP450), lipoxygenase (LOX), or cyclooxygenase (COX) pathways, or non-enzymatically via free radical peroxidation, play critical roles in regulating maternal-fetal immune tolerance, uterine

quiescence, placental vascularization, and parturition.[26–29] Disruptions in oxylipin homeostasis have been implicated in pregnancy complications, including preeclampsia, fetal growth restriction, and PTB, underscoring their significance in maternal-fetal health.[28] Free FAs and lysophospholipids can be derived from the enzymatic hydrolysis of membrane phospholipids, catalyzed by phospholipase A2.[30] FAs, in addition to serving as precursors for oxylipins, support placental function by promoting angiogenesis, cell signaling, and nutrient transport to the fetus.[29,31] Among these, omega-3 FAs, such as docosahexaenoic acid (DHA) and eicosapentaenoic acid (EPA), are particularly notable for their anti-inflammatory properties, with higher levels associated with a reduced risk of PTB.[32,33] Lysophospholipids further enhance maternal-fetal adaptation and maintain uterine homeostasis by regulating cellular migration, immune activation, and vascular remodeling.[34–36] Endocannabinoids, also derived from polyunsaturated FAs, contribute to labor onset by stimulating the production of prostaglandins PGE2 and PGF2α, which govern uterine contractions, cervical ripening, and membrane rupture.[37] Lastly, bile acids, traditionally recognized for their role in lipid metabolism, also function as immunomodulatory signaling molecules.[38] Elevated levels have been implicated in intrahepatic cholestasis of pregnancy, a condition associated with adverse pregnancy outcomes, including sPTB.[39,40] The analysis of these signaling lipid molecules in urine provides a powerful approach to investigating their association with sPTB, as urinary metabolites originate from vaginal microbiota-host interactions as well as broader systemic physiological processes.[41]

To complement the findings of our previous VOC analysis, we conducted a pilot study with 30 women presenting with imminent PTB, to investigate the potential role of signaling lipids in the pathophysiology and accurate risk stratification of sPTB. Participants were stratified into three groups based on subsequent delivery outcomes: spontaneous preterm delivery without histological evidence of chorioamnionitis, spontaneous preterm delivery with histologically confirmed chorioamnionitis, and term delivery. Specifically, the study aimed to (i) explore metabolic differences between pregnancies leading to spontaneous preterm and term deliveries, with a focus on delineating biochemical signatures associated with non-infectious and infection-driven etiologies of sPTB, and (ii) evaluate the potential of urinary metabolites as predictive non-invasive bed-side biomarkers to distinguish, at the time of suspicion, pregnant women who will actually deliver preterm from those who will eventually deliver at term. These investigations will aid in advancing our understanding of the diverse and complex mechanisms contributing to sPTB and could allow the development of more precise diagnostics tools for accurate prediction of sPTB.

2. Materials and Methods

2.1 Cohort

The study cohort presented here is a subset of a larger prospective cohort of pregnant women admitted to the maternity ward of the Department of Obstetrics at Erasmus MC Sophia Hospital in Rotterdam, the Netherlands.[19] Briefly, all participants presented with imminent PTB. Women between 23+5 and 33+6 weeks of gestation received antenatal corticosteroids and tocolytics in accordance with local clinical guidelines. For all cases of PTB, placental tissue was subjected to histopathological analysis for the confirmation of chorioamnionitis. Baseline maternal and pregnancy characteristics, as well as delivery details, were systematically retrieved from electronic patient records. The inclusion and exclusion criteria, as well as the admission protocols, have been described extensively in our previous study.[19]

2.2 Sample collection and storage

From the original prospective cohort, a subset of 30 women with gestational ages between 28+0 and 34+0 was retrospectively selected for inclusion in this pilot study (**Figure 1**). This retrospective cohort comprised 10 women who delivered spontaneously preterm without histological evidence of chorioamnionitis, 10 women who delivered spontaneously preterm with histologically confirmed chorioamnionitis, and 10 women who delivered at term, representing the three distinct clinical groups under investigation. At admission and prior to any drug treatments, 25 mL of midstream or catheterized urine was collected from each participant, which were stored at 4°C within 30 minutes in a 50 mL sterile falcon tube, and subsequently transported for long-term storage at -20°C. Selected samples were later retrieved and transferred on dry ice to the analytical chemistry laboratory, where they were stored at -20°C until aliquoting for metabolomic analysis. A 4 mL aliquot of urine was sent to the Diagnostic Core Laboratory at Erasmus MC for osmolality measurement, which was used for sample normalization in downstream analysis.

2.3 Metabolomic data acquisition

For a comprehensive analysis of signaling lipids, the clinical urine samples were analyzed using two distinct preparation protocols adapted from Yang *et al.* and Fu *et al*.: (i) a standard protocol to extract free lipids, and (ii) an enzymatic deconjugation protocol to hydrolyze glucuronidated lipids, which are conjugated with glucuronic acid to enhance their water solubility for urinary excretion.[42,43]

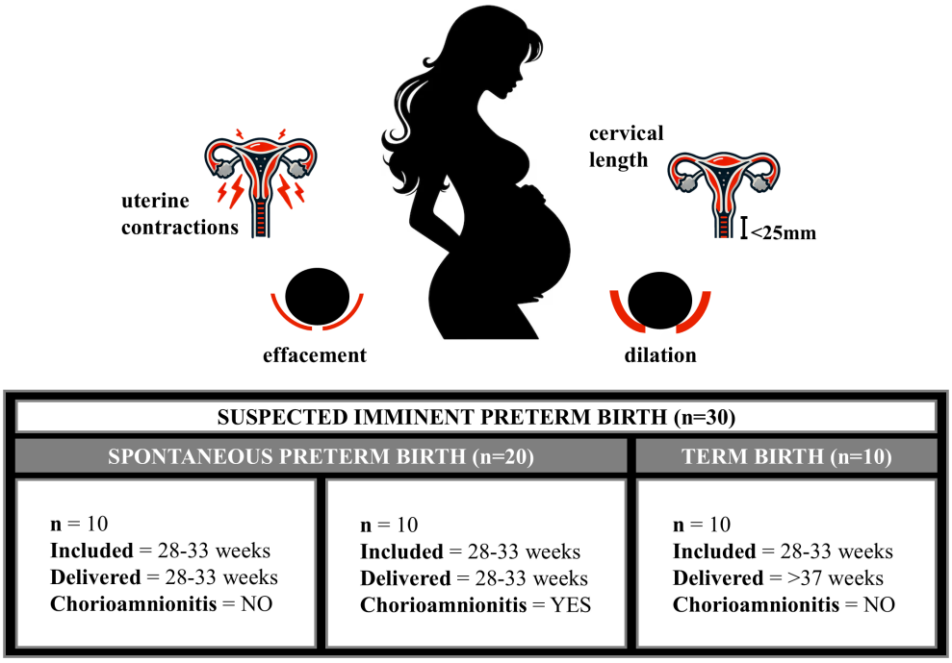

Figure 1. Overview of study design and sample classification. The figure illustrates the study design, which included 30 women presenting with suspected imminent preterm birth based on the presence of painful uterine contractions, and/or cervical length <25mm, and/or cervical effacement and dilation. Participants were categorized into three groups based on their subsequent delivery outcomes: (i) non-infectious preterm group (n=10); women who delivered preterm spontaneously without chorioamnionitis, (ii) infectious preterm group (n=10); women who delivered preterm spontaneously with chorioamnionitis, and (iii) term group (n=10); women who delivered at term.

2.3.1 Standard sample preparation

In the standard preparation, 400 µL of urine sample was spiked with 10 µL of antioxidant solution (0.2 mg mL^{-1} BHT and 0.2 mg mL^{-1} EDTA), 20 µL of internal standard (ISTD) solution composed of deuterated targets, and 200 µL of 0.2 M citric acid and 0.4 M disodium hydrogen phosphate buffer (pH 4.5). Lipids were extracted using liquid-liquid extraction using 1 mL of BuOH:MTBE (1:1 v/v). The samples were subjected to a vortexing of 1 min, followed by centrifugation at 15,800 rcf for 10 min at 4°C. A volume of 800 µL of the upper organic phase was separated, dried under vacuum using a speedVac, and reconstituted in 50 µL of 70:30 (v/v) mixture of MeOH:ACN. The samples were vortexed and centrifuged for 10 min at 4°C and at 15,800 rcf, following which they were transferred into a vial for subsequent analysis via LC-MS/MS. The detailed methodology, including chemicals and reagents, preparation of ISTD solution, and overall protocol is described in Yang *et al*.[43] While the standard protocol of Yang *et al*. remains unchanged, the volumes and matrix type were adapted based on the approach outlined by Fu *et al*.[42]

2.3.2 Enzymatic deconjugation sample preparation

To hydrolyze conjugated lipids, an additional enzymatic deconjugation step was incorporated prior to lipid extraction based on the protocol of Fu *et al*.[42] In this preparation, 400 µL of urine sample was spiked with 10 µL of antioxidant solution (0.2 mg mL^{-1} BHT and 0.2 mg mL^{-1} EDTA), 20 µL of ISTD solution, and 200 µL of enzyme solution. The enzyme solution was prepared using β-glucuronidase derived from bovine liver, dissolved in 200 mM acetate buffer at 4.5 pH, with a final enzyme concentration of 1000 units per sample. The samples were incubated at 37°C for 2h to facilitate enzymatic hydrolysis of the conjugated lipids. Following incubation, 200 µL of 0.2 M citric acid and 0.4 M disodium hydrogen phosphate buffer (pH 4.5) were added, and lipids were extracted and reconstituted as described in the standard preparation protocol.

2.3.3 Lipid analysis by LC-MS/MS

To ensure a comprehensive coverage of a wide range of compound classes, two chromatographic methods were employed, following the protocol established by Yang *et al*.[43] Briefly, a low pH chromatography was utilized for various oxylipins (such as prostaglandins, isoprostanes (iPs), hydroxyeicosatetraenoic acids (HETEs), dihydroxyeicosatetraenoic acids (DiHETEs), hydroxyoctadecadienoic acids (HODEs), epoxyeicosatrienoic acids (EpETrEs), dihydroxyeicosatrienoic acids (DiHETrEs), hydroxyeicosapentaenoic acids (HEPEs), and hydroxydocosahexaenoic acids (HDoHEs)), endocannabinoids, and bile acids, and a high pH chromatography for FAs and lysophospholipids (such as lysophosphatidic acids (LPAs), cyclic lysophosphatidic acids (cLPAs), lysophosphatidylethanolamines (LPEs), lysophosphatidylinositol (LPIs), and lysophosphatidylglycerol (LPGs)) ranging from C14 to C22 chain length species. Chromatographic separation was performed by a Shimadzu Nexera X2 LC formed by three high pressure pumps (LC-30AD), communication module (CBM-20Alite), autosampler (SIL-30AC), and an oven (CTO-30A) from Shimadzu Benelux, employing a Waters BEH C18 column (2.1 × 50 mm, 1.7 µm) for the low pH chromatography and a Kinetex EVO C18 column (2.1 × 50 mm, 1.7 µm) for the high pH chromatography. ESI-MS was conducted using a Sciex QTRAP 6500 MS for both chromatography, allowing for polarity switching and dynamic MRM. Peak integration of the acquired MRM data was performed using the vendor software Sciex OS (v2.1.6.59781).

2.4 Data preprocessing

Quality control was performed utilizing mzQuality software based on pooled study samples, method blanks, and ISTDs.[44] To account for variability in sample processing and instrument performance, peak area ratios were calculated using the closest eluting ISTD for each metabolite. The metabolite dataset was curated by selecting each metabolite from either the

standard or the enzymatic deconjugation analysis, based on the method with higher median peak area and superior peak shape and quality. Metabolites demonstrating a relative standard deviation (RSD) below 30% in pooled quality control samples and a background signal of less than 40% in method blanks were retained for downstream analysis. Fisher's exact test was applied to evaluate potential associations between missing data and experimental groups, and metabolites with over 20% missingness were excluded from subsequent analyses. Additionally, biologically pertinent metabolite ratios of product to precursor (*e.g.* 20-HETE to AA ratio) and sums of metabolites within the same subclass (*e.g.* sum of all HETEs), were computed to provide insights into enzyme activities and shifts in metabolic pathways. All metabolic data was normalized to osmolality, $\log_2$ transformed, and missing values were imputed using the Quantile Regression Imputation of Left-Censored data method.[45] The data was further auto-scaled for multivariable analysis.

2.5 Statistics

All descriptive statistics, statistical tests, and visualization were performed in RStudio (v4.3.1). Clinical cohort characteristics were summarized using median and range for continuous variables and number with percentage for categorical variables. To determine whether these variables differed significantly between the overall preterm and term groups, Welch's t-test was applied to continuous variables, and logistic regression for categorical variables. Univariate differential analysis was performed using linear regression, with metabolite as the response and a dichotomous variable representing the comparison groups as the predictor. Effect sizes of the linear regression models are provided by the model's β coefficients. Models were corrected for the study-specific statistical confounders for preterm outcome identified from the baseline clinical characteristics. The primary analysis compared the combined preterm groups to the term group, to provide an overarching assessment of preterm-associated metabolic alterations, independent of etiology. Subsequently, pairwise comparisons were conducted to examine group-specific differences: (i) preterm deliveries without chorioamnionitis versus term, (ii) preterm deliveries with chorioamnionitis versus term, and (iii) preterm deliveries with chorioamnionitis versus preterm deliveries without chorioamnionitis. Univariate and multivariable logistic regression analysis was performed using potential biomarkers identified from the univariate linear regression analysis to distinguish women who delivered preterm from those who delivered at term. Given the limited sample sizes of individual subgroups (non-infectious and infectious preterm), the overall preterm cohort was analyzed as a single group to ensure model stability and prevent overfitting. Additionally, vaginal discharge was evaluated independently as well as in combination with the metabolic models to assess their predictive performance, as it reflects changes in the vaginal microenvironment, which has been associated with preterm birth.[46]

Leave-one-out-cross-validation was used to evaluate model performances. A significance threshold of 0.05 was applied to p-values across all statistical analyses. To account for multiple testing, p-values were adjusted using Benjamini-Hochberg method implemented by the *p.adjust* function. These adjusted p-values, termed q-values, were subjected to a significance threshold of 0.1. These corrections accounted for the total number of metabolic features in univariate tests (n=133).

2.6 Ethics

The study was granted an exemption from formal ethical approval by the local institutional Medical Ethics Committee in accordance with the Dutch Medical Research involving Human Subjects Act (MEC-2018-1302). Written informed consent was obtained from all participants prior to their inclusion in the study. The research was supported by the Erasmus MC Sophia, Departments of Obstetrics and Gynecology and Neonatology, and conducted in strict adherence to the ethical principles outlined in the Code of Ethics of the World Medical Association (Declaration of Helsinki).

3. Results

3.1 Clinical cohort characteristics

A summary of key demographic and clinical characteristics is provided in **Table 1**. The gestational age at birth ranged from 29+0 to 32+5 in the preterm groups and 37+1 to 41+1 in the term group. Gestational age at the time of inclusion and collection of urinary samples was comparable across groups, ranging from 28+0 to 32+2 and reflecting uniformity in the stage of pregnancy during participant enrollment. Apart from chorioamnionitis, PTBs in this cohort were not associated with other clinical conditions commonly linked to PTB, such as urinary tract infections and pre-eclampsia. The median CRP level of the preterm group with chorioamnionitis was higher compared to the other groups, although mean differences were not statistically significant. Based on the t-test and logistic regression analysis comparing overall preterm and term groups, differences in number of prior births ($p = 0.01$), a history of miscarriages ($p = 0.03$), and presence of vaginal discharge ($p = 0.006$) were found to be significantly associated with preterm birth outcomes.

3.2 Metabolic cohort characteristics

The quality control review excluded one outlier in the term group, which was identified based on visual anomalies during chromatographic peak integration and further validated through principal component analysis. Among the 182 metabolites targeted using the two chromatographic methods, including 79 oxylipins, 64 lysophospholipids, 16 fatty acids, 8

Table 1. Demographic and clinical characteristics of the study cohort. The table presents the demographic and clinical characteristics of the pilot study dataset, including gestational age at birth and at inclusion, maternal age, BMI, ethnicity, CRP levels, number of prior births, prior preterm birth, vaginal discharge, and miscarriage history. Continuous variables are expressed as median (range), while categorical variables are reported as number (percentage). Baseline characteristics were compared between overall preterm vs term using t-test for continuous variables and logistic regression for categorical variables, with corresponding p-values provided. BMI = body mass index; CRP = C-reactive protein.

Characteristic		Dataset (n=29)					P-value
		All (n=29)	Term Birth (n=9)		Preterm Birth (n=20)		
				All (n=20)	Without Chorioamnionitis (n=10)	With Chorioamnionitis (n=10)	
Gestational Age at Birth in weeks + days [median (range)]		31+4 (29+0 - 41+1)	37+5 (37+1 - 41+1)	30+6 (29+0 - 32+5)	31+2 (29+0 - 32+5)	29+6 (29+1 - 31+1)	< 0.0001*
Maternal Age at Birth in years [median (range)]		31 (20 - 42)	32 (26 - 35)	29 (20 - 42)	30 (20 - 42)	29 (23 - 34)	0.35
Gestational Age at Inclusion in weeks + days [median (range)]		30+3 (28+0 - 32+2)	31+0 (28+0 - 31+5)	30+2 (28+0 - 32+2)	30+5 (28+1 - 32+2)	29+4 (28+0 - 32+1)	0.73
BMI in kg/m^2 [median (range)]		26 (18.40 - 46.80)	25.70 (20.20 - 46.80)	26.22 (18.40 - 42.30)	25.49 (18.4 - 33.33)	26.80 (20 - 42.3)	1
C-Reactive Protein in mg/l [median (range)]		9.5 (0.4 - 79)	11.05 (0.4 - 23)	9.5 (1.9 - 79)	7.35 (2 - 66)	14 (1.9 - 79)	0.22
Number of Prior Births [median (range)]		1 (0 - 4)	2 (0 - 4)	0 (0 -2)	0 (0 - 2)	0 (0 - 1)	0.01*
Ethnicity [n (%)]	Caucasian	13 (68.42)	3 (33.33)	10 (50)	6 (60)	4 (40)	0.29
	Non-Caucasian	9 (31.03)	4 (44.44)	5 (25)	2 (20)	3 (30)	
	Missing	7 (24.14)	2 (22.22)	5 (25)	2 (20)	3 (30)	
Prior Preterm Births [n(%)]	Yes	5 (17.24)	2 (22.22)	3 (15)	0 (0)	3 (30)	0.58
	No	22 (6.90)	6 (66.67)	16 (80)	9 (90)	7 (70)	
	Missing	2 (0)	1 (11.11)	1 (5)	1 (10)	0 (0)	
Vaginal Discharge [n (%)]	Yes	8 (27.59)	0 (0)	8 (40)	4 (40)	4 (40)	0.006*
	No	20 (68.97)	9 (100)	11 (55)	5 (50)	6 (60)	
	Missing	1 (3.45)	0 (0)	1 (5)	1 (10)	0 (0)	
Miscarriage [n (%)]	Yes	8 (27.59)	5 (55.55)	3 (15)	1 (10)	2 (20)	0.03*
	No	20 (68.97)	4 (44.44)	16 (80)	8 (80)	8 (80)	
	Missing	1 (3.45)	0 (0)	1 (5)	1 (10)	0 (0)	

bile acids, 15 endocannabinoids, and 1 steroid hormone, 102 passed the predefined acceptance thresholds. Based on the median peak area and peak quality, data of oxylipins and FAs were obtained from the enzymatic deconjugation analysis while lysophospholipids, endocannabinoids, and bile acids were derived from the standard analysis. A total of 15 metabolites exhibited varying degrees of missing data, of which three metabolites exceeding 20% missingness, were excluded from further analysis. A total of 34 derived metabolic features were computed, including 23 ratios and 11 sums, to enhance the characterization of metabolic pathways. The three statistical confounders identified in the clinical cohort

characteristics were accounted for in the linear regression models: number of prior births, miscarriages (yes/no), and vaginal discharge (yes/no).

3.3 Differential metabolic regulation in preterm and term deliveries

3.3.1 Overall preterm birth versus term birth

The univariate analysis of differential metabolic abundances between overall preterm and term deliveries revealed metabolic associations ($p<0.05$) with sPTB, identifying 13 metabolites with lower levels in the preterm group compared to the term group (**Figure 2a**). Among the 13 metabolites, 11 were oxylipins predominantly generated via the LOX and CYP450 pathways, utilizing arachidonic acid (AA), linoleic acid (LA), DHA, or EPA as precursors, while the remaining 2 metabolites were lysophospholipids. The LOX-derived metabolites included 15-HETE, HDoHEs (8-HDoHE, 10-HDoHE), and HODEs (9-HODE, sum HODEs), with β coefficients ranging from -1.42 to -0.85. Oxylipins generated via the CYP450 pathway comprised DiHETrEs (8,9-DiHETrE, 11,12-DiHETrE, 14,15-DiHETrE, sum DiHETrEs), 20-HETE, and 17,18-DiHETE (β = -1.49 to -1.04). The two lysophopholipids identified were LPA(18:2) (β = -2.04) and LPG(14:0) (β = -2.80). Detailed results of the analysis, including effect estimates and p-values for all metabolites, are provided in **Table S1**.

3.3.2 Preterm birth without chorioamnionitis versus term birth

The pairwise comparison between non-infectious sPTB and term birth revealed metabolic differences ($p<0.05$) that were similar with those identified in the overall preterm vs. term analysis (**Figure 2b**). AA-derived metabolites, including HETEs (20-HETE, sum HETEs), and DiHETrEs (5,6-DiHETrE, 8,9-DiHETrE, 11,12-DiHETrE, 14,15-DiHETrE, sum DiHETrEs) exhibited lower levels in the non-infectious preterm group (β = -2.23 to -1.30). Similar trends were observed for LA-derived HODEs (9-HODE, sum HODEs), DHA-derived 8-HDoHE, EPA-derived DiHETEs (14,15-DiHETE, 17,18-DiHETE, sum DiHETEs) and 9-HEPE (β = -1.65 to -1.23), as well as lysophospholipid LPG(14:0) (β = -3.57). Detailed results of the analysis, including effect estimates and p-values for all metabolites, are provided in **Table S2**.

3.3.3 Preterm birth with chorioamnionitis versus term birth

In the comparison between preterm deliveries with infection and term deliveries, only three metabolites were found to be lower in the infectious preterm group compared to the term group with $p<0.05$ (**Figure 2c**): 9-HODE (**Figure 2e**), sum HODEs, and 8,9-DiHETrE (β = -1.58 to -1.15). Detailed results of the analysis, including effect estimates and p-values for all metabolites, are provided in **Table S3**.

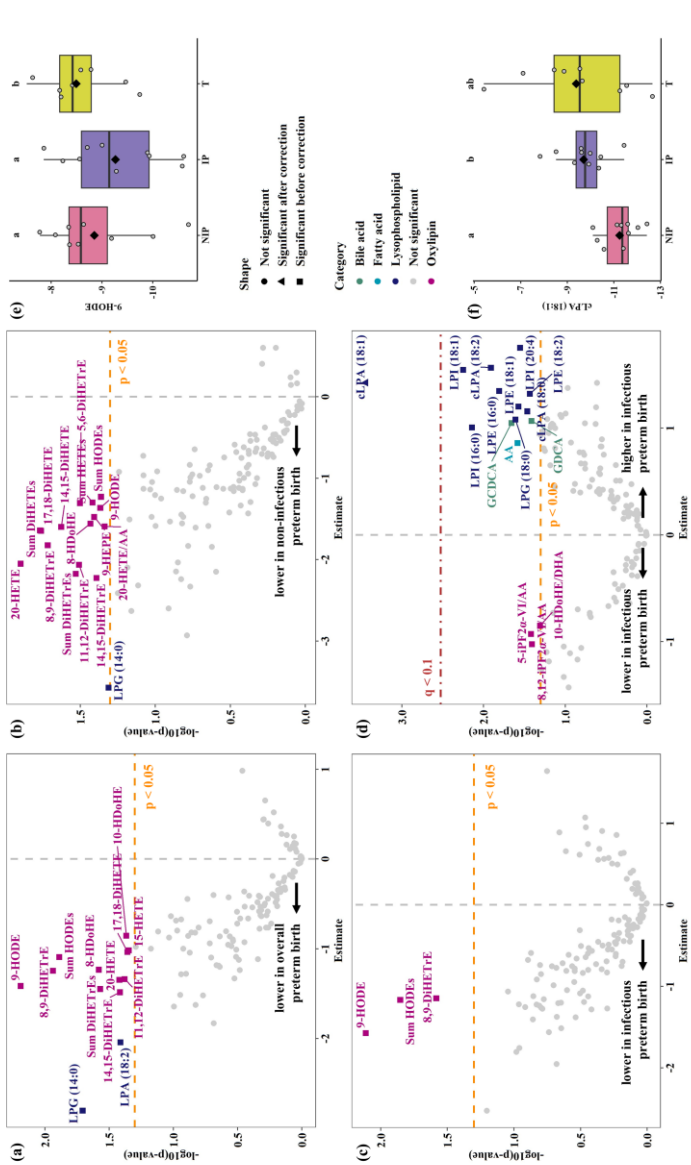

Figure 2. Differentially regulated metabolites across term and preterm births. The figure presents volcano plots and boxplots illustrating metabolite differences across study groups. Panels (a-d) display volcano plots based on univariate linear regression analysis for the following comparisons: (a) term birth vs. overall preterm birth, (b) term birth vs. non-infectious preterm birth, (c) term birth vs. infectious preterm birth, and (d) non-infectious preterm birth vs. infectious preterm birth. The x-axis represents the regression estimate and the y-axis depicts statistical significance ($-\log_{10}$ p-value). Metabolites are color-coded by compound classes, including bile acids, fatty acids, lysophospholipids, and oxylipins. Data points are shaped to indicate significance levels: significant after FDR correction, significant before FDR correction, and not significant. The vertical dashed line indicates an estimate of zero effect, and horizontal dashed lines denote significance thresholds. Panels (e) and (f) show boxplots of 9-HODE and cLPA(18:1), highlighting their distribution across study groups. In each boxplot, the central line represents the median, with box edges denoting the interquartile range. Individual data points represent samples, and the black diamond represents the mean. The letters denote significance between groups from the linear-mixed effect models: shared letters indicate no significant difference ($p>0.05$), while unique letters indicate significant difference ($p<0.05$). FDR = False Discovery Rate; IP = infectious preterm; NIP = non-infectious preterm; T = term.

3.3.4 Preterm birth without chorioamnionitis versus preterm birth with chorioamnionitis

The comparison between non-infectious and infectious preterm deliveries revealed distinct metabolic profiles, with 13 metabolites higher and 3 metabolites lower with $p<0.05$ in the infectious group compared to the non-infectious group (**Figure 2d**). Among the metabolites with higher levels, cLPAs featured prominently, including cLPA(18:0), cLPA(18:1), cLPA(18:2) (β = 1.16 to 1.57), with cLPA(18:1) (**Figure 2f**) demonstrating a statistically significant difference ($q<0.1$). Additional lysophospholipids with greater abundances included several LPIs (LPI(16:0), LPI(18:1), LPI(20:4)), LPEs (LPE(16:0), LPE(18:1), LPE(18:2)), and LPG(18:0) (β = 1.01 to 1.75). Additionally, elevated levels of AA and bile acids, glycodeoxycholic acid (GDCA) and glycochenodeoxycholic acid (GCDCA), were also observed in the infectious group (β = 0.86 to 1.07). In contrast, lower levels were observed in ratios related to oxidative stress and lipid peroxidation: 10-HDoHE/DHA, 5-iPF2α-VI/AA, and 8,12-iPF2α-VI/AA (β = -1.03 to -0.85). Detailed results of the analysis, including effect estimates and p-values for all metabolites, are provided in **Table S4**.

3.4 Predictive role of urinary signaling lipids in preterm birth

Univariate and multivariable analyses using logistic regression were performed to stratify women, at the time of clinical suspicion of imminent PTB, into those who would deliver preterm and those who would deliver at term. Predictive metabolomic models were constructed using 8,9-DiHETrE and 9-HODE, which were identified through the univariate linear regression analyses. These metabolites were selected based on their consistent identification in both non-infectious preterm vs. term and infectious preterm vs. term comparisons, suggesting their potential relevance in sPTB regardless of the underlying etiology. The predictive performance of individual models for 8,9-DiHETrE, 9-HODE, and vaginal discharge, yielded AUCs of 0.65, 0.54, and 0.58 respectively. A multivariable model with the two-metabolite panel (8,9-DiHETrE + 9-HODE), achieved an AUC of 0.61. The inclusion of vaginal discharge as an additional predictive feature in the metabolomic models enhanced performance, with AUCs increasing to 0.77 for 8,9-DiHETrE, 0.84 for 9-HODE, and 0.82 for the combined metabolite model. The most optimal model was 9-HODE + vaginal discharge, achieving an AUC of 84.2%, with a sensitivity of 73.7% and a specificity of 88.9%. Receiver operating characteristic curves and model parameters are provided in **Figure 3**.

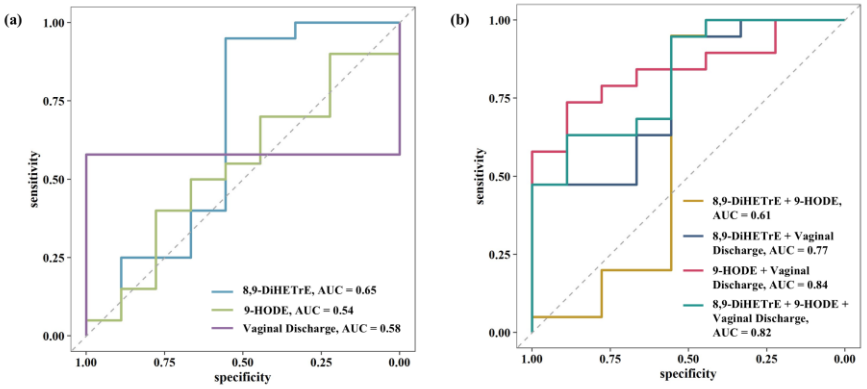

Model Type	Predictors	AUC (%)	Sensitivity (%)	Specificity (%)	Threshold
Univariate Models	8,9-DiHETrE	65.00	95.00	55.56	0.58
	9-HODE	53.89	40.00	77.78	0.74
	vaginal discharge	57.89	57.89	100.00	0.55
Multivariable Models	8,9-DiHETrE + 9-HODE	60.56	95.00	55.56	0.56
	8,9-DiHETrE + vaginal discharge	77.19	94.74	55.56	0.46
	9-HODE + vaginal discharge	84.21	73.68	88.89	0.79
	8,9-DiHETrE + 9-HODE + vaginal discharge	81.87	63.16	88.89	0.82

Figure 3. Receiver operating characteristic curves for predicting term versus preterm delivery at the moment of suspected imminent birth. The figure illustrates the diagnostic performance of predictive models in distinguishing between women who would deliver at term and those who would deliver preterm, when both are under the suspicion of imminent preterm birth. Receiver operating characteristic curves derived from leave-one-out cross-validation are shown for (a) individual models (8,9-DiHETrE, 9-HODE, vaginal discharge) and (b) multivariable models (8,9-DiHETrE + 9-HODE, 8,9-DiHETrE + vaginal discharge, 9-HODE + vaginal discharge, 8,9-DiHETrE + 9-HODE + vaginal discharge). The table presents the model parameters, including area under the curve, sensitivity, specificity, and optimal threshold. The optimal threshold refers to the probability cutoff used to classify individuals as preterm or term, determined to maximize the balance between sensitivity and specificity. DiHETrE = dihydroxyeicosatrienoic acid; HODE = hydroxyoctadecadienoic acid.

4. Discussion

Our study uniquely investigates the potential of maternal urinary signaling lipids at the moment of clinical suspicion of imminent PTB, to elucidate underlying sPTB pathophysiology and differentiate between women who will deliver preterm and those who will deliver term. Our approach captures the critical time point when interventions should be initiated, addressing a critical gap in existing predictive tools, which often fail to accurately predict pregnancy outcomes at suspicion. This inaccuracy leads to an overcautious clinical approach where some women suspected for imminent PTB are exposed to unnecessary interventions despite delivering at term leading to unintended long-term neonatal complications. Moreover, our study stratifies sPTB into non-infectious and infectious subgroups, providing deeper insights into the distinct metabolic pathways underlying these etiologies. This explorative study leveraging urinary metabolomics captures a complementary biochemical landscape against the traditional plasma or serum metabolome,

exploring its bed-side diagnostic potential to enhance accurate risk stratification and targeted interventions.

Our study highlights disruptions in oxylipin metabolism at the critical moment of clinical suspicion of imminent PTB in women who delivered preterm, providing crucial insights into potential metabolic perturbations associated with sPTB (**Figure 4**). The reduced urinary levels of several LOX- and CYP450-derived oxylipins indicate a dysregulation in pathways integral to inflammation and vascular regulation. Evidence from our study suggests that an impaired resolution of inflammation, reflected by diminished levels of anti-inflammatory mediators, may serve as a primary driver of sPTB. Specifically, the lower levels of HDoHEs, derived from omega-3 FA DHA known for its anti-inflammatory properties, may indicate an impaired anti-inflammatory response, potentially tilting the balance toward a pro-inflammatory state, a hallmark of sPTB pathophysiology and initiation of preterm labor.[47,48] This finding aligns with the clinical evidence demonstrating that supplementation of DHA reduces the risk of PTB, likely mediated through the enhanced production of protective oxylipins.[33,49] Furthermore, low plasma concentrations of EPA and DHA during pregnancy have been identified as a strong risk factor for early preterm birth in a Danish cohort, underscoring their critical role in mitigating sPTB risk.[50]

The impaired inflammation resolution is further supported by the reduced levels of DiHETrEs, which are produced through the hydrolysis of their CYP450-derived precursors, EpETrEs, by the soluble epoxide hydrolase (sEH) enzyme.[51] While EpETrEs are potent anti-inflammatory mediators, their metabolites, DiHETrEs, exhibit significantly diminished anti-inflammatory activity. Elevated levels of DiHETrEs in plasma have been reported in previous studies, which likely reflect the loss of EpETrEs' protective effects, contributing to an unresolved pro-inflammatory state driving sPTB.[52,53] In the LIFECODES birth cohort, 8,9-DiHETrE and 11,12-DiHETrE in plasma were significantly associated with increased odds of PTB.[53] Similarly, in the study by Svenvik *et al*., higher plasma levels of 11,12-DiHETrE were found to be associated with an increased risk of delivery before 34 weeks of gestation in women with preterm labor.[52] However, the reduced urinary levels of DiHETrEs observed in our study highlight a discrepancy between plasma and urinary profiles, potentially revealing a distinct spatial compartmentalization in oxylipin metabolism. Supporting this hypothesis, an animal study has shown that urinary DiHETrEs are primarily derived from the renal synthesis rather than systemic activity, as demonstrated by the negligible excretion of radio-labelled 14,15-DiHETrE in urine following plasma administration of its precursor 14,15-EpETrE.[54] This compartmentalization suggests that urinary oxylipin levels may not always be representative of systemic activity, emphasizing the need for cautious

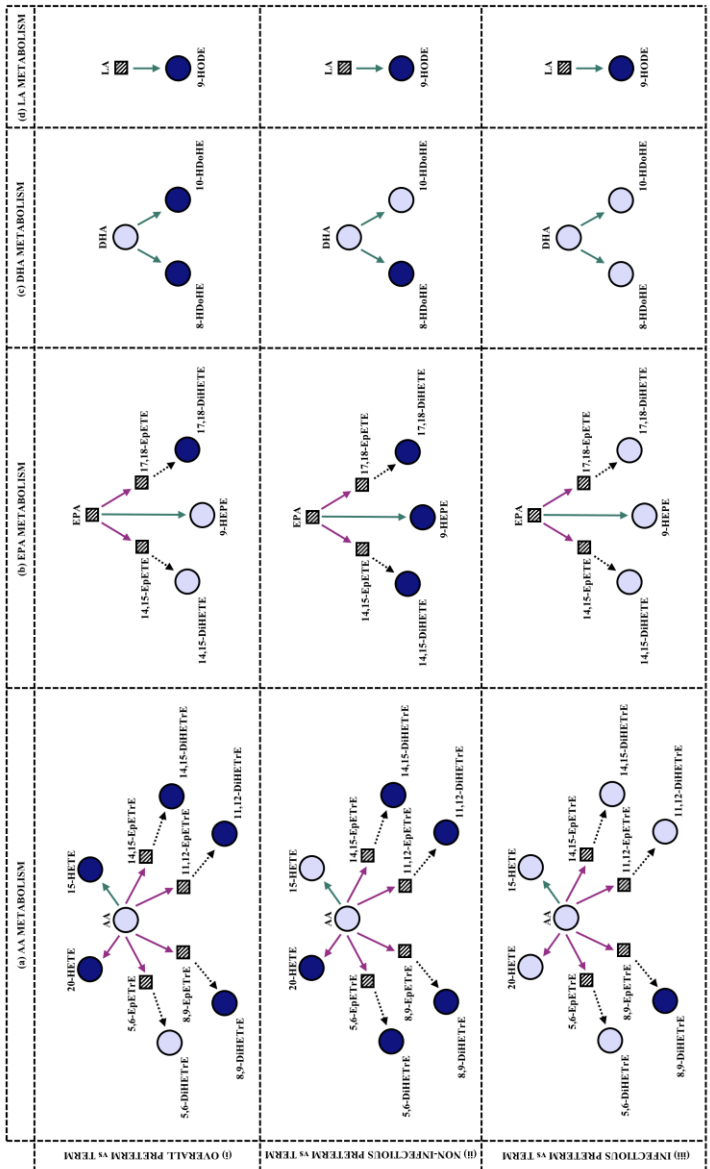

Figure 4. Network illustrating metabolic pathways, enzymes, and differential regulation of oxylipins across term and preterm births. The figure depicts the metabolic pathway of the differentially regulated oxylipins identified in this study, showing the relationships between precursors, products, and the enzymes mediating their conversion. The network illustrates the metabolism of (a) AA, (b) EPA, (c) DHA, and (d) LA. Arrows represent the enzymatic reactions mediated by the LOX, CYP450, or sEH enzymes, indicating the directionality of metabolite conversions. The network highlights the differential regulation of oxylipins across the following analyses: (i) overall preterm vs. term, (ii) non-infectious preterm vs. term, and (iii) infectious preterm vs. term. Each node represents a metabolite, color-coded to reflect its direction of regulation (upregulated or downregulated) in the preterm group compared to the term and its significance, based on univariate linear regression analysis. AA = arachidonic acid; EPA = eicosapentaenoic acid; DHA = docosahexaenoic acid; LA = linoleic acid; LOX = lipoxygenase; CYP450 = cytochrome P450; sEH = soluble epoxide hydrolase; DiHETrE = dihydroxyeicosatrienoic acid; EpETrE = epoxyeicosatrienoic acid; HETE = hydroxyeicosatetraenoic acid; DiHETE = dihydroxyeicosatetraenoic acid; EpETE = epoxyeicosatetraenoic acid; HEPE = hydroxyeicosapentaenoic acid; HDoHE = hydroxydocosahexaenoic acid; HODE = hydroxyoctadecadienoic acid.

interpretation of urinary oxylipin profiles which may be influenced by heightened systemic utilization, reduced renal synthesis, or altered excretion dynamics. Similarly, research in rats has demonstrated a significant increase in the synthesis of 20-HETE in renal tubules during the late third trimester, accompanied by a corresponding rise in its urinary excretion.[55,56] This mechanism functions to facilitate the excretion of sodium, aiding in blood pressure reduction to maintain a healthy pregnancy. The reduced urinary levels of 20-HETE observed in our study may therefore indicate an impairment in its natriuretic effect, potentially leading to increased vascular resistance and compromised placental perfusion. While placental insufficiency is well-recognized in iPTB, emerging evidence suggests it may also play a role in sPTB.[57]

The pairwise comparisons revealed that the metabolic differences observed in the overall preterm vs. term analysis were predominantly driven by the non-infectious preterm group, highlighting the unique pathophysiological mechanisms underlying non-infectious sPTB (**Figure 4**). This finding suggests that metabolomic profiling of signaling lipids could be a particularly effective tool for identifying non-infectious cases of sPTB. In contrast, the metabolic profiles of infectious preterm and term deliveries, at the moment of suspicion, exhibited less substantial differences, suggesting an activation of shared inflammatory pathways. This similarity likely stems from the overlap of mechanisms, such as production of inflammatory mediators, hormonal changes, cervical remodeling, and uterine activation, in both infection-driven preterm labor and the physiological preparation for term labor.[47,58] In term pregnancies, these processes are typically gradually initiated several weeks before birth as part of a tightly controlled physiological preparation.[59,60] However, in some women, hormonal fluctuations, transient inflammatory responses, or heightened stress, may lead to earlier cervical and uterine changes, prompting clinical suspicion of sPTB.[61] In such cases, the body may effectively compensate and resolve these triggers, allowing pregnancy to successfully progress to term. Conversely, in infection-driven sPTB, pathogen-associated molecular patterns may trigger a more rapid and intense activation of these pathways. The exaggerated inflammatory response can amplify the labor cascade beyond a critical threshold, ultimately resulting in sPTB. Therefore, alternate techniques like VOC analysis, which has shown promise in detecting infection-related sPTB, may be better suited than metabolic profiling of signaling lipids for identifying infectious sPTB at clinical suspicion. Despite this overlap, the consistent reduction in 8,9-DiHETrE and 9-HODE (**Figure 2e**) across both preterm subgroups highlights their potential as universal markers of metabolic dysregulation in sPTB, regardless of etiology. The LA-derived oxylipin, 9-HODE, serves as a natural ligand for the activation of the peroxisome proliferator-activated receptor gamma (PPARγ), a nuclear receptor known to mediate anti-inflammatory responses.[62] By modulating gene

expression, PPARγ plays a crucial role in maintaining immune homeostasis and uterine quiescence via the negative regulation of NF-kB during pregnancy.[63,64] The observed reduction in 9-HODE levels in preterm deliveries may indicate a dysregulated or impaired activation of these protective pathways, potentially contributing to the pathogenesis of sPTB.

The comparative analysis between non-infectious and infectious sPTB revealed critical insights into the mechanistic heterogeneity underlying sPTB. In the context of infectious sPTB, chorioamnionitis triggers a robust inflammatory and immune response, driven in part by the enzymatic activity of phospholipase A2.[65] The elevated levels of cLPAs (**Figure 2f**), LPIs, LPEs, and LPG observed in the infectious PTB group aligns with PLA2's role in mobilizing these lipids as part of the immune defense against pathogens. Notably, the elevated levels of cLPA, a specific and high-affinity antagonist of PPARγ, suggest an enhanced suppression of PPARγ's anti-inflammatory activity, potentially exacerbating the pro-inflammatory milieu.[66–68] Similarly, increased levels of LPI reflect its role in orchestrating immune responses to pathogenic insults, including the promotion of chemotaxis to direct immune cells to sites of inflammation and the stimulation of cytokine production.[69] Concurrently, elevated AA levels highlight its pivotal role as a precursor for pro-inflammatory lipid mediators such as prostaglandins and leukotrienes, which are integral to amplifying the inflammatory cascade and mediating immune defense mechanisms.[70] Furthermore, prostaglandins PGE2 and PGF2α, have been well documented to mediate uterine contractions and cervical ripening, processes integral to the initiation of parturition.[71] Consistent with our findings, increased levels of AA have been previously reported in blood of women who delivered preterm, which were associated with an increased sPTB risk.[72] Additionally, elevated bile acid levels observed in the infectious sPTB group suggest their involvement in PTB through enhanced oxytocin-mediated uterine contractility as bile acids have been shown to increase the expression and responsiveness of the human myometrial oxytocin receptor.[73] Supporting this observation, previous studies have demonstrated a strong correlation between serum total bile acid concentrations and increased rates of PTB, irrespective of underlying hepatic conditions.[74] In contrast, the non-infectious sPTB group exhibited heightened oxidative stress, as evidenced by elevated lipid peroxidation ratios. This finding suggests that in infectious sPTB, AA metabolism may be preferentially directed toward prostaglandin synthesis, reducing its availability for isoprostane formation. While prostaglandin-mediated pathways may primarily drive labor in infectious sPTB, oxidative stress appears to play a more prominent role in driving sPTB in the non-infectious phenotype, highlighting distinct mechanistic differences between these etiologies. Numerous studies have recognized F2 isoprostanes as biomarkers of oxidative stress which have been consistently associated with an increased likelihood of PTB.[28,75,76] Oxidative stress-induced

damage to intrauterine tissues, particularly the fetal membranes, play a pivotal role in labor initiation by promoting fetal cell senescence via the p38 MAPK pathway.[77] While this process is physiologically timed at term, premature senescence triggered by a redox imbalance is more pronounced in PTB, especially in cases involving PPROM, underscoring oxidative stress as a key mechanistic factor in the pathogenesis of sPTB.[78]

The individual predictive performance of potential metabolic biomarkers of sPTB (8,9-DiHETrE and 9-HODE), as well as vaginal discharge, demonstrated limited discriminatory power (AUCs ranging from 0.54 - 0.65) in stratifying women at the suspicion of imminent PTB based on their likelihood to deliver preterm or term. However, including vaginal discharge as an additional predictive feature with the metabolomic models significantly improved models' performances, highlighting the synergistic effect of integrating clinical observations with metabolomic data to improve risk stratification. Notably, 9-HODE + vaginal discharge emerged as the optimal model, with a high predictive performance of AUC 0.84, sensitivity 0.74, and specificity 0.89. The high specificity is particularly valuable in the clinical context, as it reduces the likelihood of unnecessary interventions in women who will ultimately deliver at term. 9-HODE reflects impaired anti-inflammatory processes driving preterm labor, while vaginal discharge likely captures localized physiological changes, such as cervical ripening, or underlying pathological conditions like infection or inflammation, underscoring its utility in complementing metabolic data.[79,80] This integrated model enables a more comprehensive assessment that accounts for both physiological and pathological processes driving preterm labor.

The design and scope of this study present several strengths and limitations that warrant consideration. A key strength lies in the homogeneity of the cohort, with participants recruited from a single center, all when admitted and treated for suspicion of PTB, ensuring consistency in clinical protocols and sample handling. The inclusion of well-characterized preterm subgroups, one with histologically confirmed chorioamnionitis and another without chorioamnionitis, facilitated the investigation of mechanistic differences underlying non-infectious and infection-driven sPTB. These findings reinforce and extend our previous VOC-based research, underscoring the multifactorial nature of sPTB and need for complementary analytical approaches to capture its diverse etiologies. The urinary metabolome offers a non-invasive tool to study lipid signaling dynamics underlying sPTB, capturing both vaginal microbiota-host interactions and systemic physiological processes. This approach provides a comprehensive view of the interconnected local vaginal environment and systemic metabolic changes contributing to sPTB risk. The small sample size of our pilot study limits the statistical power to detect subtle metabolic differences and

reduces the generalizability of the results. However, it still provides valuable preliminary insights into the mechanistic and predictive potential of urinary metabolomics in sPTB, as demonstrated by the identification of relevant biological pathways supported by existing literature. The selection of a subset from the larger cohort introduces potential selection bias, limiting the ability to detect and account for all associations with established risk factors such as prior preterm births and lifestyle variables. Additionally, vaginal discharge was self-reported by patients, which may introduce bias due to its subjective assessment and variability in individual perception. Furthermore, since urinary metabolites represent a cumulative output over time and are subject to modifications during renal filtration, reabsorption, or secretion, their systemic origin or functional role may be distorted, complicating their interpretation in the context of pathophysiological processes. Such findings underscore the necessity of integrating simultaneous plasma and urinary analyses in future studies to disentangle renal and systemic metabolic contributions, thereby strengthening mechanistic insights. To address these limitations and advance the clinical impact of this work, future research should incorporate larger, multicenter cohorts to validate the results and enhance the robustness and reliability of findings, facilitating the development of improved complementary diagnostic tools for sPTB.

5. Conclusion

sPTB remains a significant challenge in maternal and neonatal healthcare due to the interplay of multifactorial mechanisms, that hinder its timely and accurate prediction. This diagnostic uncertainty often results in the unwarranted administration of interventions at the moment of suspected imminent PTB, posing risks of adverse maternal and neonatal outcomes. Our study offers valuable insights into the underlying mechanistic pathways driving sPTB and underscores the potential of urinary signaling lipids as non-invasive biomarkers for identifying women at genuine risk at the critical moment of clinical suspicion. A pivotal insight from the study is the role of impaired resolution of inflammation as a significant driver of sPTB, as evidenced by reduced levels of anti-inflammatory mediators in urinary profiles. Moreover, our findings delineate the metabolic heterogeneity between non-infectious and infectious sPTB, with oxidative stress predominating in the former and pro-inflammatory cascades driving the latter. This mechanistic divergence emphasizes the need for phenotype-specific diagnostic approaches. Notably, urinary metabolomic profiling exhibited greater potential for distinguishing non-infectious sPTB from term deliveries, whereas infection-driven cases showed less distinct metabolic signatures likely due to activation of overlapping pathways, suggesting the potential of alternative techniques, such as VOC analysis, to enhance diagnostic precision. Furthermore, discrepancies between our urinary metabolite

findings and plasma trends reported in the literature suggest a compartmentalized metabolic response. This underscores the need for cautious interpretation of urinary metabolomic data, while also suggesting that urine may capture distinct metabolic alterations that could serve as non-invasive predictive biomarkers. This emphasizes the importance of adopting a holistic approach that accounts for contributions from different systems to comprehensively elucidate their mechanistic roles. In conclusion, this pilot study sheds light on the intricate pathophysiology of sPTB, highlighting the potential of urinary signaling lipids as biomarkers for risk stratification. This research establishes a strong foundation for future metabolomic investigations aimed at refining clinical and biochemical characteristics into diagnostic tools and developing targeted interventions, ultimately striving to enhance outcomes for women and neonates at risk of sPTB.

6. Declarations

6.1 Author contributions

Study conception: IKMR, SS, TH; Sample Collection: ER, SS; Data acquisition and curation: MUT, HLE, LL, AH; Data analysis: MUT; Data interpretation: MUT; Data visualization: MUT; Manuscript drafting: MUT, ER; Critical revision of manuscript: MUT, ER, SS, HLE, LL, AH, YBR, AF, TGJM, AK, IKMR, TH. The corresponding author attests that all listed authors meet authorship criteria and that no others meeting the criteria have been omitted.

6.2 Conflicts of Interest

The authors have declared no conflicts of interest.

7. References

1. Ohuma, E. O. *et al.* National, regional, and global estimates of preterm birth in 2020, with trends from 2010: a systematic analysis. *The Lancet* **402**, 1261–1271 (2023).
2. Rubens, C. E. *et al.* Prevention of preterm birth: Harnessing science to address the global epidemic. *Sci. Transl. Med.* **6**, (2014).
3. Goldenberg, R. L., Culhane, J. F., Iams, J. D. & Romero, R. Epidemiology and causes of preterm birth. *The Lancet* **371**, 75–84 (2008).
4. Mensah, N. A. *et al.* Examining recent trends in spontaneous and iatrogenic preterm birth across race and ethnicity in a large managed care population. *Am. J. Obstet. Gynecol.* **228**, 736.e1-736.e15 (2023).
5. Aughey, H. *et al.* Iatrogenic and spontaneous preterm birth in England: A population-based cohort study. *BJOG Int. J. Obstet. Gynaecol.* **130**, 33–41 (2023).
6. Behrman, R. E., Butler, A. S. & Outcomes, I. of M. (US) C. on U. P. B. and A. H. Causes of Preterm Birth. in *Preterm Birth: Causes, Consequences, and Prevention* (National Academies Press (US), 2007).
7. World Health Organization. *WHO Recommendations on Interventions to Improve Preterm Birth Outcomes*. (World Health Organization, Geneva, 2015).
8. Zeng, X., Jiang, W., He, X. & Zhang, J. Preterm Birth: Epidemiology, Risk Factors, Pathogenesis, and Prevention. in *Oxford Research Encyclopedia of Global Public Health* (2024). doi:10.1093/acrefore/9780190632366.013.515.
9. Hezelgrave, N. L., Shennan, A. H. & David, A. L. Tests to predict imminent delivery in threatened preterm labour. *BMJ* **350**, h2183–h2183 (2015).
10. Gravett, M. G. *et al.* Assessment of current biomarkers and interventions to identify and treat women at risk of preterm birth. *Front. Med.* **11**, (2024).
11. Ninan, K. *et al.* The proportions of term or late preterm births after exposure to early antenatal corticosteroids, and outcomes: systematic review and meta-analysis of 1.6 million infants. *The BMJ* **382**, e076035 (2023).
12. Hamm, R. F., Combs, C. A., Aghajanian, P. & Friedman, A. M. Society for Maternal-Fetal Medicine Special Statement: Quality metrics for optimal timing of antenatal corticosteroid administration. *Am. J. Obstet. Gynecol.* **226**, B2–B10 (2022).
13. Fee, E. L., Stock, S. J. & Kemp, M. W. Antenatal steroids: benefits, risks, and new insights. *J. Endocrinol.* **258**, (2023).
14. Ninan, K., Liyanage, S. K., Murphy, K. E., Asztalos, E. V. & McDonald, S. D. Evaluation of Long-term Outcomes Associated With Preterm Exposure to Antenatal Corticosteroids: A Systematic Review and Meta-analysis. *JAMA Pediatr.* **176**, e220483 (2022).
15. Melamed, N. *et al.* Neurodevelopmental disorders among term infants exposed to antenatal corticosteroids during pregnancy: a population-based study. *BMJ Open* **9**, e031197 (2019).
16. Räikkönen, K., Gissler, M. & Kajantie, E. Associations Between Maternal Antenatal Corticosteroid Treatment and Mental and Behavioral Disorders in Children. *JAMA* **323**, 1–10 (2020).
17. Haque, M. M., Merchant, M., Kumar, P. N., Dutta, A. & Mande, S. S. First-trimester vaginal microbiome diversity: A potential indicator of preterm delivery risk. *Sci. Rep.* **7**, 16145 (2017).
18. Shen, Q., Liu, Y., Li, G. & An, T. A review of disrupted biological response associated with volatile organic compound exposure: Insight into identification of biomarkers. *Sci. Total Environ.* **948**, 174924 (2024).
19. Ronde, E. *et al.* Detection of spontaneous preterm birth by maternal urinary volatile organic compound analysis: A prospective cohort study. *Front. Pediatr.* **10**, 1063248 (2022).
20. Ophelders, D. R. M. G. *et al.* Screening of Chorioamnionitis Using Volatile Organic Compound Detection in Exhaled Breath: A Pre-clinical Proof of Concept Study. *Front. Pediatr.* **9**, (2021).
21. Lacey, L., Daulton, E., Wicaksono, A., Covington, J. A. & Quenby, S. Volatile organic compound analysis, a new tool in the quest for preterm birth prediction—an observational cohort study. *Sci. Rep.* **10**, 12153 (2020).
22. Wei, S.-Q., Fraser, W. & Luo, Z.-C. Inflammatory cytokines and spontaneous preterm birth in asymptomatic women: a systematic review. *Obstet. Gynecol.* **116**, 393–401 (2010).
23. Chatterjee, P., Chiasson, V. L., Bounds, K. R. & Mitchell, B. M. Regulation of the Anti-Inflammatory Cytokines Interleukin-4 and Interleukin-10 during Pregnancy. *Front. Immunol.* **5**, 253 (2014).
24. Dutta, S., Sengupta, P. & Haque, N. Reproductive immunomodulatory functions of B cells in pregnancy. *Int. Rev. Immunol.* **39**, 53–66 (2020).
25. Boeldt, D. & Bird, I. Vascular Adaptation in Pregnancy and Endothelial Dysfunction in Preeclampsia. *J. Endocrinol.* **232**, R27–R44 (2017).
26. Liu, H. *et al.* Lipid imbalance and inflammatory oxylipin cascade at the maternal-fetal interface in recurrent spontaneous abortion. *Heliyon* **10**, e40515 (2024).
27. Mosaad, E., Peiris, H. N., Holland, O., Morean Garcia, I. & Mitchell, M. D. The Role(s) of Eicosanoids and Exosomes in Human Parturition. *Front. Physiol.* **11**, 594313 (2020).
28. Welch, B. M., McNell, E. E., Edin, M. L. & Ferguson, K. K. Inflammation and oxidative stress as mediators of the impacts of environmental exposures on human pregnancy: Evidence from oxylipins. *Pharmacol. Ther.* **239**, 108181 (2022).
29. Duttaroy, A. K. & Basak, S. Maternal dietary fatty acids and their roles in human placental development. *Prostaglandins Leukot. Essent. Fatty Acids* **155**, (2020).
30. Besenboeck, C., Cvitic, S., Lang, U., Desoye, G. & Wadsack, C. Going into labor and beyond: phospholipase A2 in pregnancy. *Reproduction* **151**, R91–R102 (2016).
31. Duttaroy, A. K. & Basak, S. Maternal Fatty Acid Metabolism in Pregnancy and Its Consequences in the Feto-Placental Development. *Front. Physiol.* **12**, (2022).
32. Fu, J. Y. *et al.* The role of omega-3 polyunsaturated fatty acids in the prevention of preterm birth. *Med. J. Aust.* **220**, (2024).
33. Cetin, I. *et al.* Omega-3 fatty acid supply in pregnancy for risk reduction of preterm and early preterm birth. *Am. J. Obstet. Gynecol. MFM* **6**, 101251 (2024).
34. Gräler, M. H. & Goetzl, E. J. Lysophospholipids and their G protein-coupled receptors in inflammation and immunity. *Biochim. Biophys. Acta BBA - Mol. Cell Biol. Lipids* **1582**, 168–174 (2002).
35. Beltrame, J. S. *et al.* Lysophosphatidic acid induces the crosstalk between the endovascular human trophoblast and endothelial cells in vitro. *J. Cell. Physiol.* **234**, 6274–6285 (2019).
36. Nagamatsu, T. *et al.* Emerging roles for lysophospholipid mediators in pregnancy. *Am. J. Reprod. Immunol. N. Y. N 1989* **72**, 182–191 (2014).
37. Chan, H.-W., McKirdy, N. C., Peiris, H. N., Rice, G. E. & Mitchell, M. D. The role of endocannabinoids in pregnancy. *Reproduction* **146**, R101–R109 (2013).
38. Fiorucci, S., Biagioli, M., Zampella, A. & Distrutti, E. Bile Acids Activated Receptors Regulate Innate Immunity. *Front. Immunol.* **9**, 1853 (2018).
39. Pataia, V., Dixon, P. H. & Williamson, C. Pregnancy and bile acid disorders. *Am. J. Physiol.-Gastrointest. Liver Physiol.* **313**, G1–G6 (2017).
40. Sarker, M., Zamudio, A. R., DeBolt, C. & Ferrara, L. Beyond stillbirth: association of intrahepatic cholestasis of pregnancy severity and adverse outcomes. *Am. J. Obstet. Gynecol.* **227**, 517.e1-517.e7 (2022).
41. Bouatra, S. *et al.* The Human Urine Metabolome. *PLoS ONE* **8**, e73076 (2013).
42. Fu, J. *et al.* Metabolomics profiling of the free and total oxidised lipids in urine by LC-MS/MS: application in patients with rheumatoid arthritis. *Anal. Bioanal. Chem.* **408**, 6307–6319 (2016).

43. Yang, W. *et al.* A comprehensive UHPLC-MS/MS method for metabolomics profiling of signaling lipids: Markers of oxidative stress, immunity and inflammation. *Anal. Chim. Acta* **1297**, 342348 (2024).
44. Peet, M. van der *et al.* mzQuality: A tool for quality monitoring and reporting of targeted mass spectrometry measurements. 2025.01.22.633547 Preprint at https://doi.org/10.1101/2025.01.22.633547 (2025).
45. Wei, R. *et al.* Missing Value Imputation Approach for Mass Spectrometry-based Metabolomics Data. *Sci. Rep.* **8**, 663 (2018).
46. Bayar, E., Bennett, P. R., Chan, D., Sykes, L. & MacIntyre, D. A. The pregnancy microbiome and preterm birth. *Semin. Immunopathol.* **42**, 487–499 (2020).
47. Romero, R. *et al.* Inflammation in preterm and term labor and delivery. *Semin. Fetal. Neonatal Med.* **11**, 317–326 (2006).
48. Habelrih, T. *et al.* Inflammatory mechanisms of preterm labor and emerging anti-inflammatory interventions. *Cytokine Growth Factor Rev.* **78**, 50–63 (2024).
49. Ramsden, C. E. *et al.* Plasma oxylipins and unesterified precursor fatty acids are altered by DHA supplementation in pregnancy: Can they help predict risk of preterm birth? *Prostaglandins Leukot. Essent. Fatty Acids* **153**, (2020).
50. Olsen, S. F. *et al.* Plasma Concentrations of Long Chain N-3 Fatty Acids in Early and Mid-Pregnancy and Risk of Early Preterm Birth. *EBioMedicine* **35**, 325–333 (2018).
51. Spector, A. A., Fang, X., Snyder, G. D. & Weintraub, N. L. Epoxyeicosatrienoic acids (EETs): metabolism and biochemical function. *Prog. Lipid Res.* **43**, 55–90 (2004).
52. Svenvik, M. *et al.* Plasma oxylipin levels associated with preterm birth in preterm labor☆. *Prostaglandins Leukot. Essent. Fatty Acids* **166**, 102251 (2021).
53. Aung, M. T. *et al.* Prediction and associations of preterm birth and its subtypes with eicosanoid enzymatic pathways and inflammatory markers. *Sci. Rep.* **9**, 17049 (2019).
54. O'Donnell, V., Milne, G., Nogueira, M., Giera, M. & Schebb, N. Quantitation of Oxylipins in Biological Samples, Focusing on Plasma, and Urine. 317–350 (2023) doi:10.1002/9783527836512.ch12.
55. Kikut, J., Komorniak, N., Ziętek, M., Palma, J. & Szczuko, M. Inflammation with the participation of arachidonic (AA) and linoleic acid (LA) derivatives (HETEs and HODEs) is necessary in the course of a normal reproductive cycle and pregnancy. *J. Reprod. Immunol.* **141**, 103177 (2020).
56. Wang, M.-H., Zand, B. A., Nasjletti, A. & Laniado-Schwartzman, M. Renal 20-hydroxyeicosatetraenoic acid synthesis during pregnancy. *Am. J. Physiol.-Regul. Integr. Comp. Physiol.* **282**, R383–R389 (2002).
57. Preston, M., Hall, M., Shennan, A. & Story, L. The role of placental insufficiency in spontaneous preterm birth: A literature review. *Eur. J. Obstet. Gynecol. Reprod. Biol.* **295**, 136–142 (2024).
58. Gonzalez, J. M., Dong, Z., Romero, R. & Girardi, G. Cervical Remodeling/Ripening at Term and Preterm Delivery: The Same Mechanism Initiated by Different Mediators and Different Effector Cells. *PLoS ONE* **6**, e26877 (2011).
59. Thornton, J. M., Browne, B. & Ramphul, M. Mechanisms and management of normal labour. *Obstet. Gynaecol. Reprod. Med.* **30**, 84–90 (2020).
60. Behrman, R. E., Butler, A. S. & Outcomes, I. of M. (US) C. on U. P. B. and A. H. Biological Pathways Leading to Preterm Birth. in *Preterm Birth: Causes, Consequences, and Prevention* (National Academies Press (US), 2007).
61. Zangeneh, F. Z. & Hantoushzadeh, S. The physiological basis with uterine myometrium contractions from electro-mechanical/hormonal myofibril function to the term and preterm labor. *Heliyon* **9**, e22259 (2023).
62. Christofides, A., Konstantinidou, E., Jani, C. & Boussiotis, V. A. The role of Peroxisome Proliferator-Activated Receptors (PPAR) in immune responses. *Metabolism.* **114**, 154338 (2021).
63. Wieser, F., Waite, L., Depoix, C. & Taylor, R. N. PPAR Action in Human Placental Development and Pregnancy and Its Complications. *PPAR Res.* **2008**, 527048 (2008).
64. Mahendra, J. *et al.* Evidence Linking the Role of Placental Expressions of PPAR-γ and NF-κB in the Pathogenesis of Preeclampsia Associated With Periodontitis. *J. Periodontol.* **87**, (2016).
65. De Luca, D. *et al.* Secretory phospholipase A2 expression and activity in preterm clinical chorioamnionitis with fetal involvement. *AJP Lung Cell. Mol. Physiol.* **323**, (2022).
66. Tsuda, S. *et al.* Cyclic phosphatidic acid is produced by autotaxin in blood. *J. Biol. Chem.* **281**, 26081–26088 (2006).
67. Tsukahara, T. *et al.* Phospholipase D2-dependent Inhibition of the Nuclear Hormone Receptor PPARγ by Cyclic Phosphatidic Acid. *Mol. Cell* **39**, 421–432 (2010).
68. Tsukahara, T. PPARγ Networks in Cell Signaling: Update and Impact of Cyclic Phosphatidic Acid. *J. Lipids* **2013**, 246597 (2013).
69. Martínez-Aguilar, L. M. *et al.* Lysophosphatidylinositol Promotes Chemotaxis and Cytokine Synthesis in Mast Cells with Differential Participation of GPR55 and CB2 Receptors. *Int. J. Mol. Sci.* **24**, 6316 (2023).
70. Dennis, E. A. & Norris, P. C. Eicosanoid Storm in Infection and Inflammation. *Nat. Rev. Immunol.* **15**, 511–523 (2015).
71. Olson, D. M. The role of prostaglandins in the initiation of parturition. *Best Pract. Res. Clin. Obstet. Gynaecol.* **17**, 717–730 (2003).
72. Reece, M. S., McGregor, J. A., Allen, K. G. & Harris, M. A. Maternal and perinatal long-chain fatty acids: possible roles in preterm birth. *Am. J. Obstet. Gynecol.* **176**, 907–914 (1997).
73. Germain, A. M. *et al.* Bile acids increase response and expression of human myometrial oxytocin receptor. *Am. J. Obstet. Gynecol.* **189**, 577–582 (2003).
74. You, S. *et al.* Dysregulation of bile acids increases the risk for preterm birth in pregnant women. *Nat. Commun.* **11**, 2111 (2020).
75. Eick, S. M. *et al.* Urinary oxidative stress biomarkers are associated with preterm birth: an ECHO program study. *Am. J. Obstet. Gynecol.* **228**, 576.e1-576.e22 (2023).
76. Ferguson, K. K., Meeker, J. D., McElrath, T. F., Mukherjee, B. & Cantonwine, D. E. Repeated measures of inflammation and oxidative stress biomarkers in preeclamptic and normotensive pregnancies. *Am. J. Obstet. Gynecol.* **216**, 527.e1-527.e9 (2017).
77. Menon, R. & Papaconstantinou, J. p38 Mitogen Activated Protein Kinase (MAPK): A New Therapeutic Target for Reducing the Risk of Adverse Pregnancy Outcomes. *Expert Opin. Ther. Targets* **20**, 1397–1412 (2016).
78. Menon, R. Oxidative Stress Damage as a Detrimental Factor in Preterm Birth Pathology. *Front. Immunol.* **5**, 567 (2014).
79. Khaskheli, M., Baloch, S., Baloch, A. S. & Shah, S. G. S. Vaginal discharge during pregnancy and associated adverse maternal and perinatal outcomes. *Pak. J. Med. Sci.* **37**, 1302–1308 (2021).
80. Becher, N., Waldorf, K. A., Hein, M. & Uldbjerg, N. The cervical mucus plug: Structured review of the literature. *Acta Obstet. Gynecol. Scand.* **88**, 502–513 (2009).

Supplementary Material

Supplementary Tables

Table S1: Linear regression model results of overall preterm vs term analysis

Metabolite	Category	Estimate (β)	Standard error	z-value	p-value	Adjusted p-value
9-HODE	Oxylipin	-1.4146	0.4726	-2.9936	0.0065	0.4612
8,9-DiHETrE	Oxylipin	-1.2447	0.4535	-2.7445	0.0115	0.4612
Sum HODEs	Oxylipin	-1.0926	0.4055	-2.6943	0.0129	0.4612
LPG (14:0)	Lysophospholipid	-2.8019	1.1174	-2.5074	0.0197	0.4612
8-HDoHE	Oxylipin	-1.2337	0.5195	-2.3746	0.0263	0.4612
Sum DiHETrEs	Oxylipin	-1.4480	0.6126	-2.3637	0.0269	0.4612
20-HETE	Oxylipin	-1.3457	0.6113	-2.2014	0.0380	0.4612
14,15-DiHETrE	Oxylipin	-1.4846	0.6761	-2.1959	0.0385	0.4612
LPA (18:2)	Lysophospholipid	-2.0420	0.9314	-2.1923	0.0387	0.4612
11,12-DiHETrE	Oxylipin	-1.3379	0.6204	-2.1566	0.0417	0.4612
10-HDoHE	Oxylipin	-0.8545	0.3989	-2.1423	0.0430	0.4612
17,18-DiHETE	Oxylipin	-1.0356	0.4858	-2.1319	0.0439	0.4612
15-HETE	Oxylipin	-1.0179	0.4803	-2.1192	0.0451	0.4612
Sum DiHETEs	Oxylipin	-0.9812	0.4765	-2.0591	0.0510	0.4844
17-HDoHE	Oxylipin	-1.0003	0.5198	-1.9245	0.0668	0.5919
Sum HETEs	Oxylipin	-0.8102	0.4361	-1.8579	0.0760	0.6100
Sum HDoHEs	Oxylipin	-0.8759	0.4986	-1.7568	0.0923	0.6100
Coriolic acid	Oxylipin	-0.6392	0.3678	-1.7377	0.0956	0.6100
LPG (18:0)	Lysophospholipid	-1.6461	0.9630	-1.7094	0.1008	0.6100
8-HETE	Oxylipin	-0.6871	0.4067	-1.6896	0.1046	0.6100
14,15-DiHETE	Oxylipin	-0.7992	0.4764	-1.6777	0.1069	0.6100
13,14-dihydro-15-keto-PGE2	Oxylipin	-1.5162	0.9191	-1.6495	0.1126	0.6100
12-HHTrE	Oxylipin	-0.6758	0.4123	-1.6393	0.1148	0.6100
9-HOTrE	Oxylipin	-1.2860	0.7845	-1.6392	0.1148	0.6100
16-HDoHE	Oxylipin	-0.9997	0.6173	-1.6194	0.1190	0.6100
13,14-dihydro-15-keto-PGF2alpha	Oxylipin	-1.2811	0.8048	-1.5917	0.1251	0.6100
Sum iPs	Oxylipin	-0.4512	0.2849	-1.5837	0.1269	0.6100
19,20-DiHDPA	Oxylipin	-0.8588	0.5469	-1.5703	0.1300	0.6100
Sum LG	Endocannabinoid	-1.0454	0.6722	-1.5551	0.1336	0.6100
11-HETE	Oxylipin	-0.8193	0.5326	-1.5384	0.1376	0.6100
omega3-DPA	Fatty acid	-0.8223	0.5480	-1.5006	0.1471	0.6183
LPG (16:0)	Lysophospholipid	-1.6268	1.0889	-1.4940	0.1488	0.6183
DALA	Fatty acid	-0.7656	0.5232	-1.4632	0.1569	0.6325
cLPA (20:4)	Lysophospholipid	-1.5198	1.0725	-1.4172	0.1698	0.6644
9-HEPE	Oxylipin	-0.6966	0.5172	-1.3468	0.1912	0.7012
Adrenic.acid	Fatty acid	-0.9418	0.6996	-1.3463	0.1913	0.7012
9(S),10(S),13(S)-TriHOME	Oxylipin	-1.0987	0.8265	-1.3294	0.1968	0.7012
8,12-iPF2α-VI	Oxylipin	-0.4024	0.3080	-1.3063	0.2044	0.7012
LPG (16:1)	Lysophospholipid	-1.8309	1.4056	-1.3026	0.2056	0.7012
cLPA (18:2)	Lysophospholipid	-1.1844	0.9320	-1.2708	0.2165	0.7097
20-HETE/AA	Oxylipin	-1.1902	0.9529	-1.2491	0.2242	0.7097
15-HETE/AA	Oxylipin	-0.8625	0.6986	-1.2347	0.2294	0.7097
alpha-12,13-DiHODE	Oxylipin	-1.2033	0.9747	-1.2346	0.2295	0.7097
DHA	Fatty acid	-0.8054	0.6917	-1.1644	0.2562	0.7584
13-HDoHE	Oxylipin	-0.9572	0.8404	-1.1390	0.2664	0.7584
5-iPF2α-VI	Oxylipin	-0.4280	0.3778	-1.1328	0.2690	0.7584
8-HDoHE/DHA	Oxylipin	-0.8625	0.7693	-1.1211	0.2738	0.7584
Sum AG	Endocannabinoid	-0.9719	0.8830	-1.1006	0.2825	0.7584
9,10-DiHOME	Oxylipin	-0.8984	0.8288	-1.0840	0.2896	0.7584
Sum DiHOMEs	Oxylipin	-0.9156	0.8453	-1.0831	0.2900	0.7584
LPE (16:1)	Lysophospholipid	-1.3329	1.2509	-1.0655	0.2977	0.7584
12,13-DiHOME	Oxylipin	-1.0924	1.0461	-1.0443	0.3072	0.7584
cLPA (18:1)	Lysophospholipid	-1.0105	0.9688	-1.0431	0.3078	0.7584
AA	Fatty acid	-0.5896	0.5697	-1.0351	0.3114	0.7584
Sum OG	Endocannabinoid	-0.7217	0.7005	-1.0302	0.3136	0.7584
13,14-dihydro-15-keto-PGF2alpha/AA	Oxylipin	-1.1257	1.1136	-1.0108	0.3226	0.7662
w3FA/w6FA	Oxylipin	-0.6634	0.6675	-0.9939	0.3306	0.7668
10-NO2-LA	Fatty acid	0.9823	1.0166	0.9663	0.3439	0.7668
8-iso-15-PGF2alpha	Oxylipin	-0.3633	0.3843	-0.9453	0.3543	0.7668
LPI (18:2)	Lysophospholipid	-1.2502	1.3228	-0.9451	0.3544	0.7668
LPE (16:0)	Lysophospholipid	-0.9280	0.9872	-0.9400	0.3570	0.7668
8-HETE/AA	Oxylipin	-0.5317	0.5662	-0.9391	0.3575	0.7668
11-HETE/AA	Oxylipin	-0.6639	0.7421	-0.8945	0.3803	0.8029

5,6-DiHETrE	Oxylipin	-0.4120	0.4680	-0.8803	0.3878	0.8060
12-HEPE	Oxylipin	-0.5010	0.6256	-0.8008	0.4314	0.8277
10-HDoHE/DHA	Oxylipin	-0.4833	0.6290	-0.7683	0.4501	0.8277
9_12_13-TriHOME	Oxylipin	-1.1181	1.4700	-0.7606	0.4546	0.8277
LPS (16:0)	Lysophospholipid	-0.4109	0.5483	-0.7495	0.4611	0.8277
LPI (16:1)	Lysophospholipid	-0.7780	1.0539	-0.7382	0.4679	0.8277
Sum HETrEs	Oxylipin	-0.5736	0.7778	-0.7374	0.4683	0.8277
11-HDoHE	Oxylipin	-0.4250	0.5811	-0.7314	0.4719	0.8277
17-HDoHE/DHA	Oxylipin	-0.6291	0.8666	-0.7260	0.4752	0.8277
15-HETrE	Oxylipin	-0.5315	0.7332	-0.7250	0.4758	0.8277
5-HETE	Oxylipin	-0.5700	0.7927	-0.7191	0.4793	0.8277
7-HDoHE	Oxylipin	-0.5712	0.7967	-0.7170	0.4806	0.8277
8-HETrE	Oxylipin	-0.6117	0.8763	-0.6980	0.4922	0.8277
Sum HEPEs	Oxylipin	-0.5024	0.7291	-0.6890	0.4977	0.8277
LPE (20:4)	Lysophospholipid	0.4371	0.6361	0.6871	0.4989	0.8277
12-HHTrE/AA	Oxylipin	-0.5204	0.7736	-0.6727	0.5079	0.8277
PGF2alpha	Oxylipin	-0.4984	0.7545	-0.6607	0.5154	0.8277
CA	Bile acid	0.6491	0.9832	0.6602	0.5157	0.8277
16-HDoHE/DHA	Oxylipin	-0.6285	0.9836	-0.6390	0.5291	0.8277
13-HDoHE/DHA	Oxylipin	-0.5860	0.9431	-0.6214	0.5405	0.8277
LPG (20:4)	Lysophospholipid	-0.7712	1.2483	-0.6178	0.5428	0.8277
5-HEPE	Oxylipin	-0.4445	0.7209	-0.6166	0.5436	0.8277
GCA	Bile acid	0.3942	0.6421	0.6140	0.5453	0.8277
LPG (18:1)	Lysophospholipid	-0.7645	1.2477	-0.6127	0.5461	0.8277
8-iso-PGF2alpha	Oxylipin	-0.2189	0.3587	-0.6103	0.5477	0.8277
LPI (20:4)	Lysophospholipid	-0.7225	1.2704	-0.5687	0.5751	0.8594
LPS (18:1)	Lysophospholipid	0.5177	0.9782	0.5292	0.6017	0.8876
cLPA (18:0)	Lysophospholipid	-0.4117	0.8024	-0.5131	0.6128	0.8876
LPI (18:1)	Lysophospholipid	-0.4863	0.9796	-0.4964	0.6243	0.8876
LPG (20:3)	Lysophospholipid	-0.5738	1.1687	-0.4909	0.6281	0.8876
5-HETE/AA	Oxylipin	-0.4146	0.8563	-0.4842	0.6328	0.8876
LPG (18:2)	Lysophospholipid	-0.4528	0.9501	-0.4766	0.6381	0.8876
PGE3	Oxylipin	0.3532	0.7468	0.4730	0.6407	0.8876
LPI (16:0)	Lysophospholipid	-0.3476	0.7521	-0.4621	0.6484	0.8890
5-iPF2α-VI/AA	Oxylipin	-0.2726	0.6058	-0.4499	0.6570	0.8895
14-HDoHE	Oxylipin	-0.3668	0.8285	-0.4428	0.6621	0.8895
LPE (18:2)	Lysophospholipid	-0.3699	0.8819	-0.4195	0.6788	0.8980
LPS (18:0)	Lysophospholipid	0.3613	0.8788	0.4112	0.6847	0.8980
18-HEPE	Oxylipin	-0.3082	0.7757	-0.3973	0.6948	0.8980
DCA	Bile acid	0.2765	0.6974	0.3964	0.6954	0.8980
8,12-iPF2α-VI/AA	Oxylipin	-0.2470	0.6771	-0.3647	0.7187	0.9185
8-iso-15-PGF2alpha/AA	Oxylipin	-0.2079	0.5983	-0.3474	0.7314	0.9185
LPE (18:1)	Lysophospholipid	-0.3170	0.9148	-0.3466	0.7321	0.9185
PGF2alpha/AA	Oxylipin	-0.3430	1.0221	-0.3356	0.7402	0.9200
Sum BA	Bile acid	0.1593	0.5132	0.3104	0.7590	0.9297
2,3-dinor-8-iso-PGF2alpha/AA	Oxylipin	0.2640	0.8611	0.3066	0.7619	0.9297
LPE (22:5)	Lysophospholipid	-0.1784	0.7079	-0.2520	0.8033	0.9684
2,3-dinor-8-iso-PGF2alpha	Oxylipin	0.1086	0.4422	0.2456	0.8082	0.9684
LPG (22:6)	Lysophospholipid	-0.1915	0.8854	-0.2163	0.8306	0.9864
7-HDoHE/DHA	Oxylipin	-0.2000	1.0196	-0.1962	0.8462	0.9874
GUDCA	Bile acid	0.1418	0.7232	0.1960	0.8463	0.9874
LPE (20:3)	Lysophospholipid	-0.1346	0.7580	-0.1776	0.8606	0.9877
LPE (22:6)	Lysophospholipid	0.1367	0.7746	0.1765	0.8614	0.9877
LPS (22:6)	Lysophospholipid	0.2414	1.5079	0.1601	0.8742	0.9906
12-HETE	Oxylipin	-0.1406	0.9378	-0.1500	0.8821	0.9906
LPI (18:0)	Lysophospholipid	0.1096	0.7808	0.1404	0.8895	0.9906
LPS (20:4)	Lysophospholipid	0.1690	1.2513	0.1351	0.8937	0.9906
8-iso-PGF2alpha/AA	Oxylipin	-0.0675	0.7337	-0.0920	0.9275	0.9962
Sum PGs	Oxylipin	0.0433	0.5077	0.0853	0.9327	0.9962
11-HDoHE/DHA	Oxylipin	-0.0538	0.6908	-0.0778	0.9386	0.9962
20-carboxy-LTB4	Oxylipin	0.0398	0.6777	0.0587	0.9537	0.9962
bicyclo-PGE2	Oxylipin	-0.0426	1.0368	-0.0411	0.9676	0.9962
LPS (18:2)	Lysophospholipid	-0.0431	1.1810	-0.0365	0.9712	0.9962
LPE (22:4)	Lysophospholipid	0.0288	1.0161	0.0284	0.9776	0.9962
12-HETE/AA	Oxylipin	0.0148	0.9163	0.0161	0.9873	0.9962
GDCA	Bile acid	0.0164	1.0516	0.0156	0.9877	0.9962
Cortisol	steroids	0.0209	1.4207	0.0147	0.9884	0.9962
LPE (18:0)	Lysophospholipid	0.0118	0.8088	0.0146	0.9884	0.9962
GCDCA	Bile acid	-0.0080	0.5974	-0.0133	0.9895	0.9962
14-HDoHE/DHA	Oxylipin	0.0044	0.9054	0.0048	0.9962	0.9962

Table S2: Linear regression model results of non-infectious preterm vs term analysis

Metabolite	Category	Estimate (β)	Standard error	z-value	p-value	Adjusted p-value
20-HETE	Oxylipin	-2.0503	0.7094	-2.8901	0.0126	0.4057
Sum DiHETEs	Oxylipin	-1.6397	0.5995	-2.7349	0.0170	0.4057
17,18-DiHETE	Oxylipin	-1.6461	0.6038	-2.7263	0.0173	0.4057
8,9-DiHETrE	Oxylipin	-1.8230	0.6820	-2.6731	0.0191	0.4057
14,15-DiHETE	Oxylipin	-1.5982	0.6233	-2.5640	0.0236	0.4057
Sum DiHETrEs	Oxylipin	-2.1748	0.8891	-2.4461	0.0294	0.4057
11,12-DiHETrE	Oxylipin	-2.0633	0.8528	-2.4193	0.0309	0.4057
5,6-DiHETrE	Oxylipin	-1.3054	0.5414	-2.4111	0.0314	0.4057
8-HDoHE	Oxylipin	-1.5582	0.6703	-2.3245	0.0369	0.4057
Sum HETEs	Oxylipin	-1.2977	0.5623	-2.3081	0.0381	0.4057
9-HEPE	Oxylipin	-1.4768	0.6439	-2.2935	0.0391	0.4057
14,15-DiHETrE	Oxylipin	-2.2263	0.9783	-2.2756	0.0404	0.4057
9-HODE	Oxylipin	-1.3636	0.6079	-2.2430	0.0430	0.4057
Sum HODEs	Oxylipin	-1.2283	0.5490	-2.2373	0.0434	0.4057
20-HETE/AA	Oxylipin	-1.5922	0.7211	-2.2079	0.0458	0.4057
LPG (14:0)	Lysophospholipid	-3.5715	1.6432	-2.1735	0.0488	0.4057
LPG (18:0)	Lysophospholipid	-2.4133	1.1507	-2.0971	0.0561	0.4223
8,12-iPF2α-VI	Oxylipin	-0.9242	0.4429	-2.0869	0.0572	0.4223
cLPA (18:2)	Lysophospholipid	-2.0984	1.0413	-2.0152	0.0650	0.4377
19,20-DiHDPA	Oxylipin	-1.5067	0.7542	-1.9977	0.0671	0.4377
LPE (16:0)	Lysophospholipid	-2.6314	1.3281	-1.9813	0.0691	0.4377
LPA (18:2)	Lysophospholipid	-2.3179	1.2054	-1.9229	0.0767	0.4403
Sum iPs	Oxylipin	-0.7254	0.3861	-1.8785	0.0829	0.4403
Coriolic acid	Oxylipin	-0.9665	0.5150	-1.8768	0.0832	0.4403
10-HDoHE	Oxylipin	-1.1316	0.6033	-1.8755	0.0834	0.4403
15-HETE	Oxylipin	-1.1399	0.6272	-1.8175	0.0923	0.4403
5-HEPE	Oxylipin	-1.4752	0.8174	-1.8047	0.0943	0.4403
8-HETE	Oxylipin	-1.0484	0.5820	-1.8015	0.0949	0.4403
11-HETE	Oxylipin	-1.2092	0.6820	-1.7731	0.0996	0.4403
5-HETE	Oxylipin	-1.5891	0.8974	-1.7707	0.1000	0.4403
8-iso-15-PGF2alpha	Oxylipin	-0.9178	0.5227	-1.7559	0.1026	0.4403
17-HDoHE	Oxylipin	-1.2516	0.7273	-1.7208	0.1090	0.4530
LPG (16:0)	Lysophospholipid	-2.6017	1.5737	-1.6532	0.1222	0.4706
LPE (18:0)	Lysophospholipid	-1.5343	0.9352	-1.6405	0.1249	0.4706
cLPA (18:1)	Lysophospholipid	-2.1462	1.3556	-1.5833	0.1374	0.4706
Sum HDoHEs	Oxylipin	-1.1461	0.7279	-1.5744	0.1394	0.4706
LPG (18:2)	Lysophospholipid	-2.0360	1.3000	-1.5662	0.1413	0.4706
13,14-dihydro-15-keto-PGE2	Oxylipin	-1.4495	0.9447	-1.5343	0.1489	0.4706
cLPA (18:0)	Lysophospholipid	-1.5551	1.0186	-1.5268	0.1508	0.4706
Sum LG	Endocannabinoid	-1.1612	0.7652	-1.5176	0.1530	0.4706
LPG (20:4)	Lysophospholipid	-2.3758	1.5660	-1.5171	0.1532	0.4706
9-HOTrE	Oxylipin	-1.4780	0.9751	-1.5157	0.1535	0.4706
LPG (20:3)	Lysophospholipid	-1.8732	1.2614	-1.4850	0.1614	0.4706
LPG (16:1)	Lysophospholipid	-2.9306	1.9784	-1.4813	0.1623	0.4706
DALA	Fatty acid	-1.0455	0.7190	-1.4541	0.1696	0.4706
5-iPF2α-VI	Oxylipin	-0.8368	0.5756	-1.4538	0.1697	0.4706
LPE (16:1)	Lysophospholipid	-2.3318	1.6088	-1.4494	0.1709	0.4706
AA	Fatty acid	-0.9904	0.6841	-1.4477	0.1714	0.4706
Adrenic.acid	Fatty acid	-0.9532	0.6667	-1.4297	0.1764	0.4706
16-HDoHE	Oxylipin	-1.2232	0.8567	-1.4278	0.1769	0.4706
12-HHTrE	Oxylipin	-0.6472	0.4597	-1.4080	0.1826	0.4746
13,14-dihydro-15-keto-PGF2alpha	Oxylipin	-1.6074	1.1499	-1.3978	0.1856	0.4746
8-HDoHE/DHA	Oxylipin	-0.9712	0.7146	-1.3590	0.1972	0.4950
DHA	Fatty acid	-1.1192	0.8422	-1.3289	0.2067	0.5092
LPE (18:2)	Lysophospholipid	-1.3020	1.0030	-1.2981	0.2168	0.5166
LPS (18:0)	Lysophospholipid	-1.2536	0.9693	-1.2932	0.2184	0.5166
GCDCA	Bile acid	-0.9021	0.7075	-1.2750	0.2246	0.5166
LPI (18:2)	Lysophospholipid	-1.5890	1.2482	-1.2731	0.2253	0.5166
omega3-DPA	Fatty acid	-0.8422	0.6697	-1.2575	0.2307	0.5200
cLPA (20:4)	Lysophospholipid	-1.8459	1.4908	-1.2382	0.2375	0.5265
LPG (18:1)	Lysophospholipid	-2.1508	1.8015	-1.1939	0.2539	0.5482
LPI (16:0)	Lysophospholipid	-1.1115	0.9344	-1.1894	0.2555	0.5482
5-HETE/AA	Oxylipin	-1.1309	1.0115	-1.1181	0.2838	0.5973
Sum BA	Bile acid	-0.7472	0.6736	-1.1093	0.2874	0.5973
Sum PGs	Oxylipin	-0.6925	0.6460	-1.0720	0.3032	0.6168
Sum HEPEs	Oxylipin	-1.1679	1.0961	-1.0654	0.3061	0.6168
LPS (18:2)	Lysophospholipid	-1.4238	1.3519	-1.0532	0.3114	0.6182
LPI (16:1)	Lysophospholipid	-1.1275	1.0859	-1.0384	0.3180	0.6220
LPI (18:1)	Lysophospholipid	-1.1094	1.1015	-1.0072	0.3322	0.6318
LPE (18:1)	Lysophospholipid	-1.1598	1.1525	-1.0063	0.3326	0.6318

8-HETE/AA	Oxylipin	-0.5903	0.5924	-0.9964	0.3373	0.6318
15-HETE/AA	Oxylipin	-0.6818	0.6972	-0.9778	0.3460	0.6392
13-HDoHE	Oxylipin	-1.1198	1.1796	-0.9493	0.3598	0.6425
PGF2alpha	Oxylipin	-1.0304	1.0918	-0.9438	0.3625	0.6425
GUDCA	Bile acid	-0.9457	1.0055	-0.9405	0.3641	0.6425
LPI (20:4)	Lysophospholipid	-1.3370	1.4406	-0.9281	0.3703	0.6425
11-HETE/AA	Oxylipin	-0.7511	0.8173	-0.9190	0.3748	0.6425
13,14-dihydro-15-keto-PGF2alpha/AA	Oxylipin	-1.1493	1.2669	-0.9071	0.3808	0.6425
alpha-12,13-DiHODE	Oxylipin	-1.1317	1.2497	-0.9056	0.3816	0.6425
7-HDoHE	Oxylipin	-0.9969	1.1209	-0.8894	0.3900	0.6483
Sum AG	Endocannabinoid	-0.9455	1.1252	-0.8403	0.4159	0.6653
17-HDoHE/DHA	Oxylipin	-0.6645	0.7957	-0.8352	0.4187	0.6653
11-HDoHE	Oxylipin	-0.7039	0.8452	-0.8328	0.4200	0.6653
8-iso-15-PGF2alpha/AA	Oxylipin	-0.4596	0.5609	-0.8194	0.4273	0.6653
10-HDoHE/DHA	Oxylipin	-0.5446	0.6688	-0.8143	0.4301	0.6653
GDCA	Bile acid	-1.2931	1.5881	-0.8142	0.4302	0.6653
LPS (22:6)	Lysophospholipid	-1.4127	1.7938	-0.7875	0.4451	0.6745
8,12-iPF2α-VI/AA	Oxylipin	-0.4661	0.6158	-0.7569	0.4626	0.6745
Sum OG	Endocannabinoid	-0.6779	0.8984	-0.7546	0.4639	0.6745
LPS (20:4)	Lysophospholipid	-1.0740	1.4261	-0.7531	0.4648	0.6745
w3FA/w6FA	Oxylipin	-0.6351	0.8584	-0.7398	0.4726	0.6745
GCA	Bile acid	-0.5299	0.7178	-0.7383	0.4735	0.6745
bicyclo-PGE2	Oxylipin	-0.8028	1.0883	-0.7377	0.4738	0.6745
LPG (22:6)	Lysophospholipid	-1.0012	1.3664	-0.7327	0.4767	0.6745
12-HEPE	Oxylipin	-0.6736	0.9429	-0.7143	0.4876	0.6827
9(S),10(S),13(S)-TriHOME	Oxylipin	-0.7044	1.0479	-0.6722	0.5132	0.7069
8-iso-PGF2alpha/AA	Oxylipin	0.4031	0.6031	0.6685	0.5155	0.7069
2,3-dinor-8-iso-PGF2alpha/AA	Oxylipin	0.6018	0.9171	0.6561	0.5232	0.7093
16-HDoHE/DHA	Oxylipin	-0.6362	0.9811	-0.6485	0.5280	0.7093
5-iPF2α-VI/AA	Oxylipin	-0.3787	0.5974	-0.6340	0.5371	0.7143
CA	Bile acid	-0.7372	1.2264	-0.6011	0.5581	0.7271
20-carboxy-LTB4	Oxylipin	-0.5470	0.9212	-0.5938	0.5628	0.7271
LPE (22:4)	Lysophospholipid	-0.6947	1.1706	-0.5934	0.5631	0.7271
LPI (18:0)	Lysophospholipid	-0.5224	0.9406	-0.5554	0.5881	0.7520
LPE (20:3)	Lysophospholipid	-0.4712	0.9021	-0.5224	0.6102	0.7569
13-HDoHE/DHA	Oxylipin	-0.5328	1.0306	-0.5170	0.6138	0.7569
12,13-DiHOME	Oxylipin	-0.7416	1.4345	-0.5170	0.6139	0.7569
LPE (22:5)	Lysophospholipid	-0.4639	0.9407	-0.4931	0.6301	0.7569
Sum HETrEs	Oxylipin	-0.5150	1.0445	-0.4931	0.6302	0.7569
8-HETrE	Oxylipin	-0.6233	1.2760	-0.4885	0.6334	0.7569
10-NO2-LA	Fatty acid	0.5995	1.2395	0.4837	0.6367	0.7569
PGF2alpha/AA	Oxylipin	-0.5723	1.1857	-0.4827	0.6374	0.7569
18-HEPE	Oxylipin	-0.5163	1.1352	-0.4548	0.6568	0.7730
12-HETE	Oxylipin	-0.5418	1.3116	-0.4131	0.6863	0.8007
LPS (16:0)	Lysophospholipid	-0.2923	0.7336	-0.3984	0.6968	0.8059
PGE3	Oxylipin	-0.2813	0.7798	-0.3607	0.7241	0.8246
LPS (18:1)	Lysophospholipid	-0.4476	1.2471	-0.3589	0.7254	0.8246
14-HDoHE	Oxylipin	-0.4217	1.2064	-0.3495	0.7323	0.8254
7-HDoHE/DHA	Oxylipin	-0.4099	1.2640	-0.3243	0.7509	0.8343
LPE (22:6)	Lysophospholipid	-0.3340	1.0378	-0.3218	0.7527	0.8343
DCA	Bile acid	-0.3273	1.0769	-0.3039	0.7660	0.8371
12-HHTrE/AA	Oxylipin	-0.1891	0.6274	-0.3014	0.7679	0.8371
15-HETrE	Oxylipin	-0.2275	0.8318	-0.2735	0.7888	0.8528
LPE (20:4)	Lysophospholipid	0.2375	0.9007	0.2637	0.7962	0.8528
2,3-dinor-8-iso-PGF2alpha	Oxylipin	0.1436	0.5598	0.2566	0.8015	0.8528
Sum DiHOMEs	Oxylipin	-0.2245	1.1563	-0.1941	0.8491	0.8962
Cortisol	steroids	0.2990	1.8478	0.1618	0.8740	0.9033
14-HDoHE/DHA	Oxylipin	0.1653	1.0829	0.1527	0.8810	0.9033
9,10-DiHOME	Oxylipin	-0.1709	1.1358	-0.1505	0.8827	0.9033
11-HDoHE/DHA	Oxylipin	-0.1169	0.7786	-0.1502	0.8829	0.9033
8-iso-PGF2alpha	Oxylipin	-0.0550	0.5046	-0.1089	0.9149	0.9289
9_12_13-TriHOME	Oxylipin	-0.1461	1.9819	-0.0737	0.9424	0.9472
12-HETE/AA	Oxylipin	-0.0837	1.2383	-0.0676	0.9472	0.9472

Table S3: Linear regression model results of infectious preterm vs term analysis

Metabolite	Category	Estimate (β)	Standard error	z-value	p-value	Adjusted p-value
9-HODE	Oxylipin	-1.5753	0.5071	-3.1064	0.0077	0.8335
Sum HODEs	Oxylipin	-1.1681	0.4164	-2.8055	0.0140	0.8335
8,9-DiHETrE	Oxylipin	-1.1477	0.4615	-2.4866	0.0261	0.8335
LPG (14:0)	Lysophospholipid	-2.5275	1.2484	-2.0246	0.0624	0.8335
8-HDoHE	Oxylipin	-1.0650	0.5846	-1.8220	0.0899	0.8335
LPA (18:2)	Lysophospholipid	-1.8065	1.0391	-1.7385	0.1041	0.8335
Sum DiHETrEs	Oxylipin	-1.2232	0.7137	-1.7139	0.1086	0.8335
13,14-dihydro-15-keto-PGE2	Oxylipin	-1.7566	1.0277	-1.7093	0.1095	0.8335
20-HETE	Oxylipin	-1.2573	0.7620	-1.6500	0.1212	0.8335
10-HDoHE	Oxylipin	-0.6793	0.4186	-1.6227	0.1269	0.8335
Coriolic acid	Oxylipin	-0.5932	0.3729	-1.5909	0.1340	0.8335
9(S),10(S),13(S)-TriHOME	Oxylipin	-1.4080	0.8964	-1.5707	0.1386	0.8335
11,12-DiHETrE	Oxylipin	-1.1215	0.7157	-1.5670	0.1394	0.8335
14,15-DiHETrE	Oxylipin	-1.2247	0.7995	-1.5318	0.1478	0.8335
17-HDoHE	Oxylipin	-0.9180	0.6000	-1.5300	0.1483	0.8335
9-HOTrE	Oxylipin	-1.2398	0.8242	-1.5042	0.1548	0.8335
12-HHTrE	Oxylipin	-0.7413	0.4952	-1.4970	0.1566	0.8335
15-HETE	Oxylipin	-0.8526	0.5739	-1.4855	0.1596	0.8335
9,10-DiHOME	Oxylipin	-1.2665	0.8529	-1.4850	0.1597	0.8335
Sum DiHOMEs	Oxylipin	-1.2757	0.8667	-1.4719	0.1632	0.8335
15-HETE/AA	Oxylipin	-1.1592	0.7949	-1.4584	0.1668	0.8335
10-NO2-LA	Fatty acid	1.6381	1.1514	1.4228	0.1767	0.8335
20-HETE/AA	Oxylipin	-1.5639	1.1159	-1.4015	0.1828	0.8335
Sum HDoHEs	Oxylipin	-0.7566	0.5522	-1.3702	0.1922	0.8335
16-HDoHE	Oxylipin	-0.9886	0.7311	-1.3522	0.1978	0.8335
17,18-DiHETE	Oxylipin	-0.7743	0.5856	-1.3222	0.2073	0.8335
9_12_13-TriHOME	Oxylipin	-1.9553	1.4821	-1.3192	0.2083	0.8335
12,13-DiHOME	Oxylipin	-1.3765	1.0464	-1.3155	0.2095	0.8335
13,14-dihydro-15-keto-PGF2alpha	Oxylipin	-1.2078	0.9291	-1.3000	0.2146	0.8335
GCA	Bile acid	0.8847	0.6870	1.2877	0.2187	0.8335
8-HDoHE/DHA	Oxylipin	-1.2014	0.9472	-1.2683	0.2254	0.8335
13,14-dihydro-15-keto-PGF2alpha/AA	Oxylipin	-1.5145	1.1942	-1.2682	0.2254	0.8335
Sum DiHETEs	Oxylipin	-0.7173	0.5736	-1.2505	0.2316	0.8335
Sum BA	Bile acid	0.6554	0.5404	1.2129	0.2452	0.8335
8-HETE/AA	Oxylipin	-0.8137	0.6731	-1.2088	0.2468	0.8335
12-HHTrE/AA	Oxylipin	-1.0479	0.8723	-1.2013	0.2496	0.8335
Sum HETEs	Oxylipin	-0.6157	0.5204	-1.1831	0.2565	0.8335
omega3-DPA	Fatty acid	-0.7561	0.6620	-1.1421	0.2726	0.8335
11-HETE/AA	Oxylipin	-0.9500	0.8504	-1.1172	0.2827	0.8335
10-HDoHE/DHA	Oxylipin	-0.8157	0.7340	-1.1113	0.2852	0.8335
w3FA/w6FA	Oxylipin	-0.7848	0.7067	-1.1105	0.2855	0.8335
cLPA (20:4)	Lysophospholipid	-1.3816	1.2548	-1.1011	0.2894	0.8335
19,20-DiHDPA	Oxylipin	-0.6611	0.6074	-1.0884	0.2948	0.8335
Sum iPs	Oxylipin	-0.3190	0.3009	-1.0603	0.3070	0.8335
GCDCA	Bile acid	0.6108	0.5797	1.0536	0.3099	0.8335
alpha-12,13-DiHODE	Oxylipin	-1.0899	1.0420	-1.0459	0.3133	0.8335
8-HETE	Oxylipin	-0.5070	0.4888	-1.0372	0.3172	0.8335
Sum LG	Endocannabinoid	-0.8368	0.8258	-1.0134	0.3281	0.8335
17-HDoHE/DHA	Oxylipin	-1.0543	1.0416	-1.0122	0.3286	0.8335
LPG (18:0)	Lysophospholipid	-1.1943	1.1963	-0.9983	0.3351	0.8335
CA	Bile acid	1.0669	1.0843	0.9839	0.3419	0.8335
11-HETE	Oxylipin	-0.6434	0.6569	-0.9794	0.3440	0.8335
LPS (18:0)	Lysophospholipid	0.9474	0.9713	0.9754	0.3459	0.8335
LPS (16:0)	Lysophospholipid	-0.5999	0.6318	-0.9496	0.3584	0.8335
GUDCA	Bile acid	0.7434	0.7838	0.9485	0.3590	0.8335
16-HDoHE/DHA	Oxylipin	-1.1249	1.1868	-0.9478	0.3593	0.8335
Adrenic.acid	Fatty acid	-0.8005	0.8447	-0.9477	0.3593	0.8335
14,15-DiHETE	Oxylipin	-0.5333	0.5677	-0.9393	0.3635	0.8335
LPG (16:0)	Lysophospholipid	-1.2863	1.4203	-0.9057	0.3804	0.8515
DALA	Fatty acid	-0.5679	0.6321	-0.8984	0.3842	0.8515
Sum OG	Endocannabinoid	-0.7295	0.8624	-0.8459	0.4118	0.8979
LPE (20:4)	Lysophospholipid	0.5476	0.6694	0.8180	0.4270	0.9035
9-HEPE	Oxylipin	-0.4560	0.5586	-0.8164	0.4280	0.9035
LPE (18:0)	Lysophospholipid	0.6841	0.8528	0.8022	0.4359	0.9058
Sum AG	Endocannabinoid	-0.7924	1.0292	-0.7700	0.4541	0.9171
LPS (18:1)	Lysophospholipid	0.9032	1.1822	0.7640	0.4576	0.9171
5-iPF2α-VI/AA	Oxylipin	-0.5015	0.6631	-0.7563	0.4620	0.9171
13-HDoHE	Oxylipin	-0.6952	0.9899	-0.7023	0.4940	0.9371
13-HDoHE/DHA	Oxylipin	-0.8315	1.1946	-0.6961	0.4978	0.9371
LPG (16:1)	Lysophospholipid	-1.2747	1.8462	-0.6905	0.5012	0.9371

DCA	Bile acid	0.5720	0.8493	0.6735	0.5116	0.9371
8,12-iPF2α-VI/AA	Oxylipin	-0.4895	0.7294	-0.6710	0.5131	0.9371
18-HEPE	Oxylipin	-0.5016	0.7543	-0.6650	0.5169	0.9371
8,12-iPF2α-VI	Oxylipin	-0.1828	0.2907	-0.6289	0.5396	0.9371
8-HETrE	Oxylipin	-0.5499	0.8811	-0.6240	0.5426	0.9371
12-HEPE	Oxylipin	-0.4028	0.6491	-0.6206	0.5448	0.9371
LPE (22:6)	Lysophospholipid	0.5026	0.8108	0.6199	0.5453	0.9371
8-iso-PGF2alpha/AA	Oxylipin	-0.5039	0.8543	-0.5898	0.5647	0.9371
Sum HETrEs	Oxylipin	-0.4634	0.7988	-0.5801	0.5711	0.9371
PGF2alpha/AA	Oxylipin	-0.6331	1.1131	-0.5688	0.5785	0.9371
cLPA (18:2)	Lysophospholipid	-0.6033	1.0655	-0.5663	0.5802	0.9371
15-HETrE	Oxylipin	-0.4747	0.8458	-0.5612	0.5835	0.9371
LPS (22:6)	Lysophospholipid	0.8524	1.5393	0.5538	0.5885	0.9371
LPI (18:0)	Lysophospholipid	0.4925	0.9089	0.5419	0.5964	0.9371
DHA	Fatty acid	-0.4184	0.7815	-0.5354	0.6007	0.9371
5-iPF2α-VI	Oxylipin	-0.1948	0.3726	-0.5229	0.6092	0.9371
8-iso-15-PGF2alpha/AA	Oxylipin	-0.3492	0.6749	-0.5173	0.6130	0.9371
8-iso-PGF2alpha	Oxylipin	-0.1916	0.3800	-0.5043	0.6219	0.9385
GDCA	Bile acid	0.6257	1.2878	0.4859	0.6346	0.9385
LPI (18:2)	Lysophospholipid	-0.8061	1.7184	-0.4691	0.6462	0.9385
LPE (16:1)	Lysophospholipid	-0.7020	1.5283	-0.4594	0.6530	0.9385
LPS (20:4)	Lysophospholipid	0.6332	1.4316	0.4423	0.6650	0.9385
14-HDoHE/DHA	Oxylipin	-0.4476	1.0138	-0.4415	0.6656	0.9385
PGE3	Oxylipin	0.3990	0.9209	0.4333	0.6714	0.9385
cLPA (18:0)	Lysophospholipid	0.3148	0.7996	0.3937	0.6997	0.9385
AA	Fatty acid	-0.2481	0.6546	-0.3790	0.7104	0.9385
PGF2alpha	Oxylipin	-0.3264	0.8717	-0.3745	0.7137	0.9385
5-HETE/AA	Oxylipin	-0.3698	0.9882	-0.3742	0.7138	0.9385
14-HDoHE	Oxylipin	-0.3113	0.8640	-0.3603	0.7240	0.9385
5,6-DiHETrE	Oxylipin	-0.1875	0.5255	-0.3567	0.7266	0.9385
LPI (16:1)	Lysophospholipid	-0.4532	1.3311	-0.3405	0.7386	0.9385
cLPA (18:1)	Lysophospholipid	-0.3916	1.1651	-0.3361	0.7418	0.9385
Sum PGs	Oxylipin	0.1714	0.5147	0.3329	0.7441	0.9385
LPE (22:4)	Lysophospholipid	0.3885	1.1874	0.3272	0.7484	0.9385
Sum HEPEs	Oxylipin	-0.2629	0.8228	-0.3195	0.7541	0.9385
5-HEPE	Oxylipin	-0.2586	0.8120	-0.3185	0.7548	0.9385
7-HDoHE/DHA	Oxylipin	-0.3822	1.2014	-0.3182	0.7551	0.9385
12-HETE/AA	Oxylipin	-0.2916	1.0309	-0.2829	0.7814	0.9505
LPS (18:2)	Lysophospholipid	0.4147	1.4707	0.2820	0.7821	0.9505
7-HDoHE	Oxylipin	-0.2459	0.8891	-0.2766	0.7861	0.9505
LPG (22:6)	Lysophospholipid	0.2591	1.0584	0.2448	0.8102	0.9552
2,3-dinor-8-iso-PGF2alpha	Oxylipin	0.1303	0.5587	0.2333	0.8189	0.9552
20-carboxy-LTB4	Oxylipin	0.1486	0.6625	0.2242	0.8258	0.9552
LPI (16:0)	Lysophospholipid	0.1788	0.8509	0.2102	0.8366	0.9552
Cortisol	steroids	-0.2779	1.3444	-0.2067	0.8392	0.9552
bicyclo-PGE2	Oxylipin	0.2144	1.1204	0.1914	0.8510	0.9552
LPG (18:2)	Lysophospholipid	0.2056	1.1131	0.1848	0.8561	0.9552
LPE (20:3)	Lysophospholipid	0.1557	0.8512	0.1829	0.8575	0.9552
2,3-dinor-8-iso-PGF2alpha/AA	Oxylipin	-0.1763	0.9654	-0.1827	0.8577	0.9552
LPE (18:2)	Lysophospholipid	0.1585	0.9274	0.1709	0.8668	0.9552
LPG (20:3)	Lysophospholipid	0.2209	1.3863	0.1593	0.8757	0.9552
LPE (16:0)	Lysophospholipid	-0.1615	1.0558	-0.1530	0.8806	0.9552
11-HDoHE/DHA	Oxylipin	-0.1265	0.8614	-0.1468	0.8854	0.9552
LPE (18:1)	Lysophospholipid	0.1305	1.0445	0.1250	0.9023	0.9552
8-iso-15-PGF2alpha	Oxylipin	-0.0425	0.3644	-0.1166	0.9088	0.9552
LPG (20:4)	Lysophospholipid	-0.1678	1.4489	-0.1158	0.9094	0.9552
LPE (22:5)	Lysophospholipid	-0.0825	0.7337	-0.1124	0.9121	0.9552
LPG (18:1)	Lysophospholipid	-0.1597	1.6174	-0.0987	0.9227	0.9570
LPI (20:4)	Lysophospholipid	-0.1424	1.5629	-0.0911	0.9287	0.9570
LPI (18:1)	Lysophospholipid	0.0932	1.1300	0.0825	0.9355	0.9570
5-HETE	Oxylipin	-0.0631	0.9181	-0.0688	0.9461	0.9606
11-HDoHE	Oxylipin	0.0098	0.5541	0.0177	0.9861	0.9886
12-HETE	Oxylipin	0.0150	1.0285	0.0146	0.9886	0.9886

Table S4: Linear regression model results of non-infectious preterm vs infectious preterm analysis

Metabolite	Category	Estimate (β)	Standard error	z-value	p-value	Adjusted p-value
cLPA (18:1)	Lysophospholipid	1.4248	0.3050	4.6708	0.0004	0.0480
LPI (18:1)	Lysophospholipid	1.5468	0.4734	3.2670	0.0056	0.2945
LPI (16:0)	Lysophospholipid	1.0057	0.3202	3.1407	0.0072	0.2945
cLPA (18:2)	Lysophospholipid	1.5657	0.5451	2.8720	0.0123	0.2945
LPE (16:0)	Lysophospholipid	1.3475	0.4891	2.7549	0.0155	0.2945
GCDCA	Bile acid	1.0472	0.4064	2.5768	0.0219	0.2945
LPG (18:0)	Lysophospholipid	1.0800	0.4289	2.5182	0.0246	0.2945
AA	Fatty acid	0.8612	0.3462	2.4874	0.0261	0.2945
LPE (18:1)	Lysophospholipid	1.2017	0.4859	2.4731	0.0268	0.2945
LPI (20:4)	Lysophospholipid	1.7528	0.7154	2.4502	0.0280	0.2945
cLPA (18:0)	Lysophospholipid	1.1575	0.4938	2.3442	0.0343	0.2945
LPE (18:2)	Lysophospholipid	1.3214	0.5732	2.3052	0.0370	0.2945
5-iPF2α-VI/AA	Oxylipin	-0.9289	0.4060	-2.2880	0.0382	0.2945
GDCA	Bile acid	1.0677	0.4680	2.2814	0.0387	0.2945
8,12-iPF2α-VI/AA	Oxylipin	-1.0251	0.4505	-2.2756	0.0391	0.2945
10-HDoHE/DHA	Oxylipin	-0.8513	0.3952	-2.1539	0.0492	0.2945
DHA	Fatty acid	0.9330	0.4353	2.1435	0.0501	0.2945
2,3-dinor-8-iso-PGF2alpha/AA	Oxylipin	-1.2614	0.5910	-2.1345	0.0510	0.2945
LPG (18:2)	Lysophospholipid	0.9714	0.4600	2.1115	0.0532	0.2945
Sum LG	Endocannabinoid	0.8100	0.3860	2.0988	0.0545	0.2945
11-HDoHE	Oxylipin	0.7854	0.3773	2.0817	0.0562	0.2945
8-iso-PGF2alpha/AA	Oxylipin	-1.1104	0.5416	-2.0504	0.0595	0.2945
LPI (16:1)	Lysophospholipid	1.0833	0.5294	2.0460	0.0600	0.2945
LPG (16:1)	Lysophospholipid	0.9534	0.4715	2.0221	0.0627	0.2945
12-HHTrE/AA	Oxylipin	-1.1858	0.5867	-2.0211	0.0628	0.2945
Sum BA	Bile acid	0.6509	0.3260	1.9966	0.0657	0.2945
LPE (20:3)	Lysophospholipid	1.0052	0.5041	1.9940	0.0660	0.2945
LPE (22:6)	Lysophospholipid	1.0285	0.5179	1.9861	0.0670	0.2945
LPE (18:0)	Lysophospholipid	1.0408	0.5289	1.9679	0.0692	0.2945
8-HETE/AA	Oxylipin	-0.7308	0.3739	-1.9546	0.0709	0.2945
5-HETE	Oxylipin	1.0286	0.5268	1.9524	0.0712	0.2945
8-HETE	Oxylipin	0.4452	0.2313	1.9249	0.0748	0.2945
LPI (18:0)	Lysophospholipid	0.8112	0.4222	1.9215	0.0753	0.2945
Sum AG	Endocannabinoid	0.9996	0.5203	1.9213	0.0753	0.2945
LPE (16:1)	Lysophospholipid	1.1219	0.6092	1.8416	0.0868	0.3299
LPS (18:1)	Lysophospholipid	1.1024	0.6048	1.8227	0.0898	0.3316
20-HETE/AA	Oxylipin	-1.3324	0.7462	-1.7855	0.0958	0.3357
17-HDoHE/DHA	Oxylipin	-1.0476	0.5869	-1.7850	0.0959	0.3357
LPE (22:4)	Lysophospholipid	1.1360	0.6463	1.7576	0.1006	0.3432
13,14-dihydro-15-keto-PGF2alpha/AA	Oxylipin	-1.4307	0.8384	-1.7064	0.1100	0.3658
16-HDoHE/DHA	Oxylipin	-1.1109	0.6591	-1.6855	0.1140	0.3700
LPG (18:1)	Lysophospholipid	0.8630	0.5176	1.6673	0.1177	0.3726
Sum HETEs	Oxylipin	0.4121	0.2525	1.6319	0.1250	0.3866
8-iso-15-PGF2alpha	Oxylipin	0.4764	0.2968	1.6050	0.1308	0.3954
PGF2alpha/AA	Oxylipin	-1.1690	0.7494	-1.5599	0.1411	0.4097
8-iso-15-PGF2alpha/AA	Oxylipin	-0.6996	0.4492	-1.5573	0.1417	0.4097
LPE (22:5)	Lysophospholipid	0.7717	0.5056	1.5264	0.1492	0.4154
10-HDoHE	Oxylipin	0.3965	0.2619	1.5140	0.1523	0.4154
LPE (20:4)	Lysophospholipid	0.6689	0.4459	1.5001	0.1558	0.4154
14-HDoHE/DHA	Oxylipin	-1.0608	0.7078	-1.4987	0.1562	0.4154
7-HDoHE	Oxylipin	0.7709	0.5270	1.4628	0.1656	0.4313
Adrenic.acid	Fatty acid	0.7493	0.5180	1.4464	0.1701	0.4313
LPG (22:6)	Lysophospholipid	0.6652	0.4641	1.4332	0.1737	0.4313
LPG (16:0)	Lysophospholipid	0.6190	0.4333	1.4284	0.1751	0.4313
DALA	Fatty acid	0.4493	0.3326	1.3509	0.1982	0.4666
8-HDoHE/DHA	Oxylipin	-0.7318	0.5435	-1.3465	0.1995	0.4666
11-HETE/AA	Oxylipin	-0.7499	0.5575	-1.3452	0.2000	0.4666
15-HETE/AA	Oxylipin	-0.7711	0.5794	-1.3309	0.2045	0.4689
LPI (18:2)	Lysophospholipid	1.2100	0.9219	1.3125	0.2105	0.4719
8-HDoHE	Oxylipin	0.5159	0.3953	1.3052	0.2129	0.4719
LPS (22:6)	Lysophospholipid	1.5159	1.2020	1.2611	0.2279	0.4961
LPS (18:2)	Lysophospholipid	1.0385	0.8374	1.2401	0.2353	0.4961
LPG (20:3)	Lysophospholipid	1.0007	0.8124	1.2318	0.2383	0.4961
LPS (20:4)	Lysophospholipid	1.1956	0.9715	1.2307	0.2387	0.4961
15-HETE	Oxylipin	0.4048	0.3339	1.2126	0.2454	0.5009
LPG (20:4)	Lysophospholipid	0.9157	0.7710	1.1877	0.2547	0.5009
11-HETE	Oxylipin	0.4260	0.3614	1.1789	0.2581	0.5009
GCA	Bile acid	0.5817	0.4951	1.1749	0.2596	0.5009
5,6-DiHETrE	Oxylipin	0.3822	0.3279	1.1654	0.2633	0.5009
GUDCA	Bile acid	0.5673	0.4900	1.1576	0.2664	0.5009

13-HDoHE	Oxylipin	0.6212	0.5378	1.1550	0.2674	0.5009
cLPA (20:4)	Lysophospholipid	0.8271	0.7307	1.1319	0.2767	0.5111
10-NO2-LA	Fatty acid	0.8953	0.7979	1.1220	0.2807	0.5115
DCA	Bile acid	0.4218	0.3826	1.1025	0.2888	0.5191
LPA (18:2)	Lysophospholipid	0.7498	0.6897	1.0872	0.2953	0.5237
12-HETE/AA	Oxylipin	-0.6686	0.6746	-0.9911	0.3384	0.5923
Sum HDoHEs	Oxylipin	0.3392	0.3575	0.9488	0.3588	0.6197
14,15-DiHETrE	Oxylipin	0.4102	0.4374	0.9380	0.3642	0.6209
Sum DiHETrEs	Oxylipin	0.3672	0.3964	0.9263	0.3700	0.6229
17,18-DiHETE	Oxylipin	0.3353	0.3658	0.9166	0.3749	0.6232
LPS (16:0)	Lysophospholipid	-0.3505	0.3956	-0.8860	0.3906	0.6290
Sum DiHETEs	Oxylipin	0.3094	0.3506	0.8827	0.3923	0.6290
5-iPF2α-VI	Oxylipin	0.2471	0.2803	0.8816	0.3929	0.6290
9(S),10(S),13(S)-TriHOME	Oxylipin	-0.5905	0.6762	-0.8733	0.3973	0.6290
11-HDoHE/DHA	Oxylipin	-0.4623	0.5402	-0.8558	0.4065	0.6351
CA	Bile acid	0.6521	0.7805	0.8355	0.4175	0.6351
12-HETE	Oxylipin	0.5073	0.6095	0.8323	0.4192	0.6351
13-HDoHE/DHA	Oxylipin	-0.6265	0.7545	-0.8304	0.4202	0.6351
omega3-DPA	Fatty acid	0.3324	0.4100	0.8106	0.4312	0.6443
11,12-DiHETrE	Oxylipin	0.3469	0.4365	0.7947	0.4400	0.6503
9-HOTrE	Oxylipin	-0.5105	0.6536	-0.7811	0.4477	0.6544
LPS (18:0)	Lysophospholipid	0.5070	0.6795	0.7462	0.4679	0.6764
Sum PGs	Oxylipin	0.2841	0.4020	0.7067	0.4914	0.7027
7-HDoHE/DHA	Oxylipin	-0.4768	0.6999	-0.6813	0.5068	0.7171
8,12-iPF2α-VI	Oxylipin	0.1508	0.2260	0.6674	0.5154	0.7215
14,15-DiHETE	Oxylipin	0.2064	0.3221	0.6409	0.5319	0.7370
w3FA/w6FA	Oxylipin	-0.3340	0.5490	-0.6085	0.5526	0.7577
Sum OG	Endocannabinoid	0.2698	0.4505	0.5988	0.5589	0.7585
9-HODE	Oxylipin	-0.2254	0.3882	-0.5806	0.5707	0.7612
Sum HETrEs	Oxylipin	0.3548	0.6136	0.5782	0.5723	0.7612
9-HEPE	Oxylipin	0.2239	0.3971	0.5637	0.5819	0.7662
8,9-DiHETrE	Oxylipin	0.1707	0.3115	0.5480	0.5924	0.7715
17-HDoHE	Oxylipin	0.2001	0.3704	0.5403	0.5975	0.7715
Cortisol	steroids	-0.6415	1.2437	-0.5158	0.6141	0.7853
19,20-DiHDPA	Oxylipin	0.2035	0.4061	0.5011	0.6241	0.7905
15-HETrE	Oxylipin	0.2776	0.5869	0.4730	0.6435	0.7942
13,14-dihydro-15-keto-PGF2alpha	Oxylipin	-0.2547	0.5469	-0.4657	0.6486	0.7942
bicyclo-PGE2	Oxylipin	0.4613	1.0015	0.4606	0.6521	0.7942
alpha-12,13-DiHODE	Oxylipin	-0.3782	0.8276	-0.4570	0.6547	0.7942
9,10-DiHOME	Oxylipin	-0.3053	0.6725	-0.4539	0.6569	0.7942
Sum DiHOMEs	Oxylipin	-0.2798	0.6933	-0.4036	0.6926	0.8299
20-HETE	Oxylipin	-0.1565	0.4537	-0.3449	0.7353	0.8697
14-HDoHE	Oxylipin	0.1869	0.5826	0.3208	0.7531	0.8697
16-HDoHE	Oxylipin	0.1368	0.4345	0.3150	0.7574	0.8697
9_12_13-TriHOME	Oxylipin	-0.3874	1.2670	-0.3058	0.7643	0.8697
12-HEPE	Oxylipin	0.1269	0.4335	0.2927	0.7740	0.8697
Coriolic acid	Oxylipin	0.0853	0.3002	0.2842	0.7804	0.8697
Sum HODEs	Oxylipin	-0.0942	0.3410	-0.2762	0.7864	0.8697
8-HETrE	Oxylipin	0.1811	0.6791	0.2667	0.7936	0.8697
2,3-dinor-8-iso-PGF2alpha	Oxylipin	-0.0854	0.3206	-0.2665	0.7937	0.8697
18-HEPE	Oxylipin	-0.1623	0.6179	-0.2627	0.7966	0.8697
LPG (14:0)	Lysophospholipid	0.1954	0.7482	0.2611	0.7978	0.8697
5-HETE/AA	Oxylipin	-0.1474	0.6181	-0.2385	0.8150	0.8748
8-iso-PGF2alpha	Oxylipin	0.0680	0.2863	0.2376	0.8156	0.8748
Sum iPs	Oxylipin	0.0452	0.2259	0.1999	0.8444	0.8985
Sum HEPEs	Oxylipin	-0.0515	0.4980	-0.1035	0.9191	0.9701
12,13-DiHOME	Oxylipin	-0.0851	0.9045	-0.0941	0.9264	0.9702
13,14-dihydro-15-keto-PGE2	Oxylipin	0.0260	0.8768	0.0296	0.9768	0.9993
12-HHTrE	Oxylipin	-0.0099	0.3492	-0.0283	0.9779	0.9993
20-carboxy-LTB4	Oxylipin	0.0125	0.5185	0.0240	0.9812	0.9993
PGF2alpha	Oxylipin	0.0069	0.5049	0.0138	0.9892	0.9993
5-HEPE	Oxylipin	-0.0050	0.5507	-0.0090	0.9930	0.9993
PGE3	Oxylipin	0.0005	0.6251	0.0009	0.9993	0.9993